METABOLIC REGULATION IN EXERCISING HIGH ALTITUDE DEER MICE

CHANGES IN METABOLIC REGULATION OF THE CARBOHYDRATE OXIDATIVE PATHWAY IN EXERCISING HIGH ALTITUDE DEER MICE

By Soren Z Coulson, B.Sc.

A Thesis Submitted to the School of Graduate Studies in Partial Fulfilment of the Requirements for the Degree Master of Science

Descriptive Note

McMaster University MASTER OF SCIENCE (2019) Hamilton, Ontario (Biology)

TITLE: Changes in metabolic regulation of the carbohydrate oxidative pathway in exercising high altitude deer mice AUTHOR: Soren Z Coulson, B.Sc. (McMaster University) SUPERVISOR: Professor G.B. McClelland NUMBER OF PAGES: xii, 80

Lay abstract

At high altitude, oxygen availability is low and can be challenging for active animals. Preferential carbohydrate oxidation is a metabolic strategy used by high altitude-native deer mice to fuel exercise because of its high energy yield per oxygen consumed. Despite the increase in carbohydrate breakdown, the capacity for muscles to use carbohydrates did not change, suggesting that the regulation of this metabolic pathway may be changing instead. We measured the contributions of two proteins involved in carbohydrate metabolism in active muscle, pyruvate dehydrogenase (PDH) and glucose transporter 4 (GLUT4), at different muscle workloads and after acclimation to high altitude conditions. We found no differences in GLUT4 content, but PDH activity was higher in hypoxia-acclimated mice at similar intensities, indicating increased rates of carbohydrate breakdown after acclimation. These data suggest that the regulation of the carbohydrate metabolic pathway changes with acclimation to support higher rates of carbohydrate oxidation during exercise.

Abstract

Hypoxia encountered at high altitude (HA) can limit energy production via aerobic metabolism in animals. Carbohydrate oxidation (CHO) has a greater ATP yield/mole O_2 than fat oxidation, and HA-native deer mice show an increased reliance on CHO during submaximal exercise after hypoxia acclimation as an O_2-saving strategy. However, hypoxia acclimation does not increase glycolytic capacity in muscle. We therefore tested the hypothesis that altered metabolic regulation of the CHO pathway allows HA mice to achieve higher rates of CHO during submaximal exercise. The objective of our study was to identify the effects of hypoxia acclimation on the regulation of two key proteins in the CHO pathway and their activation with exercise. Using first generation (G_1) laboratory born and raised HA deer mice acclimated to normoxia or chronic hypoxia, we examined the metabolic regulation of muscle glucose uptake by glucose transporter (GLUT) 4 and of pyruvate oxidation by pyruvate dehydrogenase (PDH). The gastrocnemius was electrically stimulated *in situ* under anaesthesia and acute normoxia at two submaximal workloads relative to maximal force production, which was measured using a force transducer. In frozen gastrocnemius following stimulation or rest, GLUT4 protein content was measured via Western blotting of the sarcolemmal membrane fraction and PDH activity was measured using a radiolabelled assay. We found no differences in sarcolemmal GLUT4 content with stimulation, but PDH activity was increased in hypoxia, indicating increased rates of carbohydrate breakdown at similar workloads after acclimation. These data were compared to data from wild HA deer mice sampled at their native altitude. In support of our hypothesis, these data show that the metabolic regulation of the carbohydrate oxidative

pathway changes with acclimation to support higher CHO rates during submaximal exercise. These data will help uncover the mechanistic underpinnings responsible for the exercise fuel use strategies observed exclusively in HA-native mice.

Acknowledgements

The two years of my life spent preparing this thesis have been equally challenging and fulfilling. My successes likely would not have been possible without the support of many people that I've had the pleasure to interact with during my time at McMaster. First, I would like to thank my parents, Jane and Soren, for all of their support and patience over these past few years at McMaster. Next, I would like to thank Grant for the opportunity to undertake this project and for all of the support, wisdom and patience provided throughout my thesis. I would also like to thank Graham and Marty for their insights and advice during their tenure on my supervisory committee. A special thank you goes to Dr. Sandra Peters for all of your help in troubleshooting the PDH activity assay. I sincerely appreciate all of the e-mail correspondence and your day visit to our lab; they went a long way in developing the assay. Many friends and colleagues assisted me with training in various techniques. In brief: Nicole Pranckevicius – training and optimization of the Aurora *in situ* stimulation protocol; Oliver Wearing – training in anaesthesia and surgical techniques; Cayleih Robertson – Western blotting; Katarina Djuric – collection of muscle metabolite data; Sulayman Lyons – training of the Aurora, subcellular fractionation. I would also like to thank Catie Ivy for her help in developing the acute hypoxia *in situ* stimulation protocol and for her work in maintaining the breeding colony. I would also like to thank the remaining members of the McScottland lab and the many friends I've made through the Biology Graduate Student Society, our weekly trivia team and the karate club at McMaster. It was in your company that I could celebrate my successes and forget about my setbacks.

TABLE OF CONTENTS

List of Figures and Tables

List of All Abbreviations and Symbols

ADP	Adenosine Diphosphate
AMPK	AMP-Activated Protein Kinase
ANOVA	Analysis of Variance
ATP	Adenosine-5'-Triphosphate
CHO	Carbohydrate Oxidation
CoA	Coenzyme A
Cr	Creatine
CrP	Creatine Phosphate
CS	Citrate Synthase
GLUT	Glucose Transporter
GOT	Glutamic Oxalacetic Transaminase
G6PDH	Glucose-6-Phosphate Dehydrogenase
HA	High Altitude
HIF	Hypoxia Inducible Factor
HOAD	3-Hydroxyacyl-CoA Dehydrogenase
LDH	Lactate Dehydrogenase
MCT	Monocarboxylate Transporter
MDH	Malate Dehydrogenase
NAD	β-Nicotinamide Dinucleotide
PAGE	Polyacrylamide Gel Electrophoresis
PDC	Pyruvate Dehydrogenase Complex
PDH	Pyruvate Dehydrogenase

PDK	Pyruvate Dehydrogenase Kinase
PDP	Pyruvate Dehydrogenase Phosphatase
PFK	Phosphofructokinase
PK	Pyruvate Kinase
PVDF	Polyvinylidene Fluoride
SDS	Sodium Dodecylsulfate
TCA	Tricarboxylic Acid
TEA	Triethanolamine
TPP	Thiamine Pyrophosphate
VO_2max	Maximal Rate of Oxygen Uptake

Declaration of Academic Achievement

Soren Z Coulson contributed to this thesis by conducting a majority of the data collection, experimental design and manuscript writing. Grant McClelland contributed to experimental design and manuscript revision. Katarina Djuric conducted data collection for muscle metabolites (see Chapter 2). Sulayman Lyons contributed to manuscript revision. Wild deer mouse tissue was collected at Mount Evans, CO (4300m a.s.l.) by Cayleih Robertson, Sulayman Lyons, and Grant McClelland.

CHAPTER 1: General Introduction

Background

Skeletal muscle is an important tissue to animal physiology because it makes up a large proportion of body mass and its function impacts various processes, including locomotion and shivering thermogenesis. Contractile and metabolic characteristics of muscle can vary greatly between animals of different species or even between populations in different environments. Since muscle plays a large role in a variety of activities necessary for survival in the wild, muscle phenotype is likely under intense natural selection. One such phenotype is the ability to maintain energetic balance in conditions that limit energy supply, such as in extreme environments. Despite intense stress, animals are found flourishing in a wide range of challenging conditions in the wild. Animals native to these extreme environments are likely to have evolved adaptations that allow them to sustain elevated rates of energetic output, despite limitations in energetic supply. Currently, the bioenergetics of animals native to extreme environments have not been extensively studied, presenting a ripe area of research that will contribute to the evolution and understanding of specialized metabolic phenotypes.

Coupling of Energetic Supply and Demand

A vital component to maintaining homeostasis in animals is the ability to match energetic demands with energetic supply. When an animal is performing an energetically demanding activity, rates of O_2 and substrate supply to mitochondria increase to match the elevated energetic demands of active tissue (Hochachka, 1985; Hochachka and Matheson, 1992). If energy supply is unable to meet energetic demands, then energetic output will fall

to rates that match energetic supply. A decrease in energetic output in active tissue translates to reduced performance in a variety of activities, such as locomotion (Lau et al., 2017) or thermoregulation (Meyer et al., 2010), which may result in death of the individual animal. At times, energetic balance is difficult to maintain due to variations in either or both energy demand and energy supply. For example, at high altitude, energetic demand may be elevated via increased thermogenic demand and energetic supply may be constrained by low O_2 availability. Since many activities vital to survival require sustained elevations in energetic provisioning, the ability to maintain energetic balance despite limitations in energetic supply is likely under selection.

Regulation of Metabolism

Metabolic pathway flux rates are plastic and change to meet the needs of active tissue *in vivo* (Weber, 2011; Weber and Haman, 2004). Changes in flux rate may be initiated by a myriad of intracellular and extracellular mechanisms that drive changes in pathway flux through mass action or by changes in individual protein activity. Differences in protein activity that contribute to alterations in pathway flux rates may be explained by amount of enzyme present (hierarchical regulation) or by the intracellular milieu that determines enzyme activity (metabolic regulation) (Suarez and Moyes, 2012). Both modes of regulation act on all enzymes, but the degree of control exerted by each varies between enzymes, even within the same pathway (Suarez et al., 2005). Control over pathway flux rate is distributed among all steps in that pathway, but some steps have a higher degree of control than others (Kacser et al., 1995). Steps with a high degree of control over pathway flux are important sites of flux regulation, therefore, becoming targets that modulate

metabolic phenotype. The metabolic phenotype of tissues such as skeletal muscle is plastic in response to chronic (e.g., environmental) or intermittent (e.g., exercise) energetic stress, where metabolic pathway(s) are remodeled to better mitigate bouts of energetic stress.

Mammalian Fuel Selection Patterns

A classical characteristic of any exercise bout is an acute, yet large increase in metabolic rate compared to rest. Most of this increase in energetic demand can be explained by elevated rates of ATP hydrolysis by myosin- and Ca^{2+}-ATPases in contracting muscle (Hochachka and Matheson, 1992). In response, rates of energetic supply are also elevated in exercising muscle by acutely increasing fuel oxidation rates. In the post-absorptive state, the two predominant fuels oxidized by exercising muscle in mammals are carbohydrates and lipids (Weber, 2011). Creatine phosphate (CrP) and proteins typically serve as minor ATP sources during exercise in fasted individuals, as CrP is reserved for short term intense exercise (Trump et al., 1996), while proteins are mainly oxidized in the fed state (Rennie et al., 1981). The relative contribution of lipid versus carbohydrate oxidation is dependent on exercise intensity, relative to maximal O_2 uptake (VO_2max). As workload intensities increase toward 100% VO_2max, the proportion of aerobic metabolism fueled by carbohydrates increases, while the proportion fueled by lipids decreases (Schippers et al., 2014; Weber, 2011). Preferential carbohydrate oxidation at these intense workloads occurs due to higher rates of mobilization and oxidation relative to lipids, and the capacity for anaerobic ATP production via glycolysis at workloads where O_2 delivery becomes limiting (Weber and Haman, 2004). This relationship between fuel use and $\%VO_2max$ is strongly

conserved across a wide range of mammalian taxa that differ in body size and exercise capacity (McClelland et al., 2017; Schippers et al., 2014).

Fuel Metabolism at High Altitude

High altitude environments represent a uniquely challenging niche for animals due to low ambient temperatures and barometric pressure. These two characteristics are stressful to animals, because high thermogenic output is required to defend body temperature against the ambient cold, but low barometric pressures decrease O_2 availability required for aerobic metabolism. Indeed, VO_2max in hypoxia is ~67.5 to 75% of normoxic values in lowland mice (Lui et al., 2015). By lowering VO_2max, the scope for increasing aerobic metabolic rates may be constrained, which is critical for many energetically demanding activities required for survival, including thermoregulation and exercise. Despite the challenges of life at high altitude, many species have been successful in invading this ecological niche. Animals that are native to the high alpine have survived many generations under strong selective pressure. As a result, highland animals are likely to have developed multiple adaptations to survive at high altitude, such as the ability to mitigate the suppressing effects of hypobaric hypoxia on aerobic metabolism (McClelland and Scott, 2019).

The North American deer mouse (*Peromyscus maniculatus*) is an excellent model organism to study high altitude adaptation. Deer mice have established genetically distinct populations across an altitudinal range of ~4300m, the widest of all North American mammals (Natarajan et al., 2015). Past work has identified a myriad of adaptations in deer mice from a highland population that mitigate chronic cold and hypoxic insult and promote performance in hypoxic conditions (McClelland and Scott, 2019). One such adaptation in highland deer mice is an elevated reliance on CHO during submaximal exercise in hypoxia (Lau et al., 2017), likely due to a higher ATP yield per O_2 for glucose than lipids (Brand, 2005; Welch et al., 2007). This adaptation has also been found in highland species of *Phyllotis* mice in the Peruvian Andes, when compared to lowland congenerics (Schippers et al., 2012), suggesting that elevated CHO reliance during submaximal exercise in hypoxia is conserved among highland taxa. Interestingly, these differences in carbohydrate reliance were observed when lowlanders and highlanders exercised at similar submaximal workloads (75% VO_2max), which has been shown to be a reliable predictor of fuel metabolism (Schippers et al., 2014; Weber and Haman, 2004). It is presently unclear how these highland mice rely more on CHO at submaximal exercise intensities as an exception to the mammalian fuel selection model and why this phenomenon has only been observed in highland taxa.

As an organ with function significant to exercise metabolism, skeletal muscle phenotype has been hypothesized to be a key explanatory factor for changes in whole-animal performance (Weibel and Hoppeler, 2005). Changes in muscle phenotype may manifest as changes in morphology and/or metabolic function. Despite an increase in

carbohydrate reliance with hypoxia acclimation (Lau et al., 2017), highland deer mouse gastrocnemius tissue displays a remarkable lack of plasticity in multiple traits that contribute to aerobic metabolism: capillarity, fibre type (Lui et al., 2015) and mitochondrial volume (Mahalingam et al., 2017) are all unaffected by hypoxia acclimation in the highland mice gastrocnemius. Furthermore, flux capacities at multiple steps of glycolysis and aerobic oxidation in muscle are unchanged with acclimation (Lau et al., 2017). These findings do not appear to be limited to deer mice; similar glycolytic enzyme activities were seen in highland and lowland species of *Phyllotis* mice despite large differences in exercise CHO (Schippers et al., 2012). These findings suggest that changes in hierarchical regulation with acclimation to chronic hypoxia are insufficient to explain differences in whole-animal fuel use. An alternative mechanism that has not been explored is it is differences in metabolic regulation that allow for elevated CHO pathway flux rates during submaximal exercise.

Glucose Metabolism in Exercising Muscle

Pyruvate Oxidation

A critical step to the aerobic CHO pathway is the oxidation of glycolysis-derived pyruvate to acetyl-CoA, in a series of reactions catalyzed by the pyruvate dehydrogenase complex (PDC; Equation 1). The acetyl-CoA produced by PDC may be used as a TCA cycle substrate, thus the PDC reaction serves as the linking step between glycolysis and aerobic CHO. Pyruvate oxidation is a particularly important step in aerobic CHO, as the decarboxylation step makes the PDC reaction irreversible, thus committing substrate to the aerobic pathway. Indeed, PDC activation has been shown to be a significant modulator of aerobic CHO rates and influences insulin sensitivity, therefore influencing muscle glucose uptake (Rahimi et al., 2014). As CHO rates increase with workload intensity, PDC activation follows a similar correlation (Howlett et al., 1998), consistent with the mammalian fuel selection model (Weber, 2011)

$$\text{Pyruvate} + \text{CoASH} + \text{NAD}^+ \xrightarrow{PDC} \text{Acetyl-CoA} + \text{NADH} + \text{H}^+ + \text{CO}_2 \quad (1)$$

PDC is a protein complex localized to the mitochondrial matrix and comprised of 3 subunits (E1-3) that each catalyze 1 of 3 reactions in pyruvate oxidation (reviewed by Harris et al., 2002). Since the PDC reaction acts as a gatekeeping step in aerobic CHO, PDC activity is tightly regulated to maintain appropriate flux rates. Pyruvate dehydrogenase (E1; PDH) catalyzes the pyruvate decarboxylation step and its activity strongly determines flux rates through the rest of the complex (Modak et al., 2002). PDH is covalently regulated via reversible phosphorylation at three sites of its α subunit and this

phosphorylation state directly determines PDH activity (Linn et al., 1969; Yeaman et al., 1978). PDH phosphorylation is determined by the competing activities of PDH kinases (PDK; inactivating) and phosphatases (PDP; activating). PDK expression has significant effects on fuel selection patterns in contracting muscle (Dunford et al., 2011; Herbst et al., 2012), and has been hypothesized to mediate fuel cross-talk (Sugden et al., 2001). In addition, PDK expression is plastic *in vivo* and changes in response to nutritional and hormonal signalling, thus acting as a modulator of fuel metabolism in active tissues (reviewed by Harris et al., 2002).

PDH activation is determined by the relative activities of PDK and PDP, which are extensively regulated to match PDH flux rates with metabolic demands of the tissue. The primary regulatory mechanisms for PDK and PDP activity are allosteric: the binding of an effector molecule to a site other than the active site of a protein to induce a conformational change (Guarnera and Berezovsky, 2016). Both PDK and PDP are regulated allosterically by markers of cellular energy balance, redox state and free ion concentrations. PDK is stimulated by Equation 1 product abundance (low CoASH:acetyl-CoA, NAD^+:NADH, ADP:ATP ratios) and *vice versa* (Pettit et al., 1975). In contrast, PDP is stimulated by Equation 1 substrate abundance and accumulation of Ca^{2+} (Denton et al., 1972; Pettit et al., 1975). Equation 1 substrate accumulation is mainly determined via flux rates through glycolysis and Equation 1 product accumulation is determined by tricarboxylic acid (TCA) cycle flux rates. In resting muscle, flux rates through glycolysis and TCA cycle are low, resulting in Equation 1 substrate scarcity and product abundance, respectively. Therefore, PDK activity is stimulated and PDP activity is inhibited to decrease PDH activity in resting

conditions. Conversely, flux rates through glycolysis and TCA cycle are high in exercising muscle, resulting in Equation 1 substrate abundance and product scarcity, respectively. In addition, Ca^{2+} levels are increased via crossbridge cycling in contracting muscle. Under these conditions, PDK is inhibited and PDP is stimulated during exercise, resulting in PDH activation by dephosphorylation (reviewed by Spriet and Heigenhauser, 2002).

Muscle Glucose Uptake

In mammals, glucose serves as the predominant carbohydrate oxidized to fuel metabolic processes in muscle. Two glucose sources are available to active muscle: extracellular glucose transported to muscle via circulation and intracellular glucose stored as intramuscular glycogen. Circulating glucose makes a significant contribution of substrate to the aerobic CHO pathway in exercising muscle at a wide range of submaximal workloads. As workloads increase toward 100% VO_2max, the proportion of CHO in active muscle fuelled by circulating glucose decreases, while reliance on intramuscular glycogen increases (Taylor et al., 1996).

Glucose enters muscle in a series of steps termed muscle glucose uptake (MGU) and is finely regulated to maintain glucose homeostasis (Wasserman, 2008). First, plasma glucose arrives at active muscle via the circulatory system, originating from the digestive tract (fed state) or liver (post-absorptive). Next, glucose diffuses down a concentration gradient into the muscle via facilitated diffusion through sarcolemma-embedded glucose transporters (GLUTs). Finally, glucose is phosphorylated by hexokinase to form glucose-6-phosphate, effectively trapping glucose within the muscle and maintaining an inward

glucose concentration gradient (Wasserman et al., 2011). Glucose-6-phosphate may be utilized to form glycogen (at rest) or oxidized via glycolysis to form ATP.

MGU rates are higher in exercising muscle compared to resting due to increased flux rates at each step of MGU. During exercise, plasma glucose concentrations are relatively unchanged from rest, but blood flow to active muscle increases, increasing glucose delivery rates. Exercise induces acute translocation of GLUT4 from intramuscular vesicles to the sarcolemma, increasing membrane permeability for glucose diffusion into the muscle (James et al., 1988). Presently, the mechanism for exercise-induced GLUT4 translocation is incompletely understood, but is mediated by multiple intracellular signal transduction pathways (Sylow et al., 2017). Elevated glycolytic rates in contracting muscle reduce glucose-6-phosphate accumulation, thereby increasing hexokinase activity and glucose phosphorylation rates. Previous transgenic studies have investigated the contributions of individual steps in the MGU pathway and have identified membrane glucose transport via GLUT4 to be strongly rate-determining in resting muscle (Fueger et al., 2004a; Fueger et al., 2004b). During exercise, however, MGU rates are mainly determined by the capacity of the glucose phosphorylation step, as partial GLUT4 ablation does not change MGU, but hexokinase overexpression increases MGU (Fueger et al., 2004a). It is not surprising, then, that glucose phosphorylation capacity in muscle is a determinant of endurance exercise performance (Fueger et al., 2005).

Objectives and Hypotheses

The objective of this study is to identify the effects of chronic hypoxia on the metabolic regulation of proteins in the aerobic CHO pathway in highland deer mice. The aim of this study is to provide a mechanistic explanation for the increased carbohydrate use during exercise at high altitude. I hypothesize that hypoxia acclimation alters the regulation of key proteins in the aerobic CHO pathway, changing activation kinetics with exercise intensity.

CHAPTER 2: Changes in metabolic regulation of the carbohydrate oxidative pathway in muscle of high altitude-native deer mice

Abstract

High altitude-native deer mice mitigate the suppressing effects of hypobaric hypoxia by increasing reliance on carbohydrate oxidation (CHO) to fuel submaximal exercise as an O_2-saving strategy. However, hypoxia acclimation does not increase glycolytic capacity in muscle. We therefore test the hypothesis that altered metabolic regulation of proteins in the CHO pathway allows highland mice to achieve higher CHO rates during submaximal exercise. We examined the metabolic regulation of muscle glucose uptake by glucose transporter (GLUT) 4 and pyruvate oxidation by pyruvate dehydrogenase (PDH) in wild and first generation (G_1) lab born and raised highland deer mice. Wild mice were trapped and sampled immediately post-run (75%VO_2max) at high altitude (4300m a.s.l.) and exercise was simulated *in situ* for the G_1 mice following acclimation to normoxia or chronic hypoxia. The gastrocnemius was electrically stimulated under anaesthesia and acute normoxia at two workloads relative to maximal force production. Both proteins were measured *in vitro* via quantifying sarcolemmal GLUT4 via Western blot and PDH activity using a radiolabelled assay. Surprisingly, we found no differences in sarcolemmal GLUT4 content, suggesting maximal translocation at the lower submaximal intensity. PDH activity was increased in hypoxia, indicating increased rates of carbohydrate breakdown after acclimation at similar workloads. In support of our hypothesis, these data show that the metabolic regulation of the carbohydrate oxidative pathway changes with acclimation to support higher rates of carbohydrate oxidation during

submaximal exercise. These data are the first in providing a mechanistic explanation for the whole-animal exercise fuel use strategies observed at high altitude.

Introduction

Hypobaric hypoxia is an unremitting stressor at high altitude that constrains aerobic performance in animals by decreasing O_2 availability. Despite low O_2 availability, animals are required to sustain high ATP turnover rates to fuel energetically demanding activities necessary for survival, such as exercise. Active tissues meet the elevated energetic demands of challenging activities by maintaining adequate rates of O_2 and substrate delivery to the mitochondria for ATP production via oxidative phosphorylation. Despite the challenges of high altitude, many animal species flourish in the high alpine. These animals likely have adaptations (such as elevated thermogenic capacity (Hayes and O'Connor, 1999)) that facilitate high rates of energetic output at high altitude.

An increased reliance on carbohydrate oxidation (CHO) has been hypothesized as a beneficial metabolic adaptation to high altitude due to a higher ATP yield per mole of O_2 compared to lipids (Brand, 2005; Welch et al., 2007). Our previous study found that highland deer mice (*Peromyscus maniculatus*) have a greater reliance on carbohydrates than lowland conspecifics when fuelling submaximal exercise in hypoxic conditions (Lau et al., 2017), similar to findings in highland *Phyllotis* mice from the Peruvian Andes (Schippers et al., 2012). An increase in carbohydrate use may result from increased flux rates through the CHO pathway by elevating maximum flux capacities of individual steps in the pathway (changes in hierarchical regulation) and/or by altering the regulation of individual proteins in the pathway (changes in metabolic regulation). Past work has found

limited evidence for the former hypothesis as hypoxia acclimation increased capacity for muscle glucose uptake (MGU), but not markers of glycolytic capacity in highland deer mice (Lau et al., 2017). Alternatively, flux rates through the CHO pathway could be elevated with hypoxia acclimation via changes in metabolic regulation to allow for elevated protein activation during submaximal exercise, a mechanism that has not been fully investigated in past studies.

During exercise, active muscle increases provisioning of glucose to the mitochondria by increasing rates of uptake from the circulation. MGU is elevated in active muscle via acute translocation of GLUT4 from cytosolic vesicles to the sarcolemma in response to contractions (Goodyear et al., 1990; Goodyear et al., 1991). GLUT4 is a facilitative transporter of glucose and increases in sarcolemmal GLUT4 density elevate sarcolemmal permeability to glucose. After entering the muscle, glucose is progressively oxidized in a series of ATP-yielding reactions via glycolysis in the cytosol and the TCA cycle in the mitochondria. Circulating glucose serves as a major fuel source for active muscle during submaximal exercise, but its relative contribution to total fuel metabolism decreases at relatively intense workloads (Weber et al., 1996). While highland deer mice increased reliance on CHO with hypoxia acclimation to fuel submaximal exercise, intramuscular glycogen depletion was similar between normoxia and hypoxia (Lau et al., 2017), indicating a shift in reliance toward circulating glucose at submaximal intensities.

The pyruvate dehydrogenase complex is a 3-subunit (E1-3) complex localized to the mitochondrial matrix that catalyzes the decarboxylation of pyruvate to form acetyl-CoA, acting as the linking step between glycolysis and the TCA cycle. Pyruvate dehydrogenase (PDH; E1) activity is determined by reversible phosphorylation at three sites of the α subunit (Linn et al., 1969; Yeaman et al., 1978) and is strongly rate-determining for flux rates through the entire complex (Modak et al., 2002). The phosphorylation state of PDH is determined by the competing activities of PDH kinase (PDK) and phosphatase (PDP), which are regulated allosterically by cellular redox and energy balance (Pettit et al., 1975). Since the PDH reaction is irreversible and determines the entry of glucose-derived carbon into the TCA cycle, PDH activity is tightly controlled and is a major site of metabolic regulation in CHO. Indeed, past transgenic studies that knock out PDK expression have found significant perturbations in glucose metabolism in exercising and recovering skeletal muscle (Herbst et al., 2014; Jeoung and Harris, 2008; Rahimi et al., 2014). Therefore, alterations in the regulation of PDH activity with hypoxia acclimation may contribute to the elevated CHO reliance during submaximal exercise in hypoxia (Lau et al., 2017).

The aim of this study is to provide a mechanistic explanation for increased reliance on CHO observed during whole-animal submaximal exercise and to investigate the underlying causes of the plasticity seen with acclimation to chronic hypoxia. We hypothesize that metabolic regulation of proteins in the carbohydrate oxidative pathway change with hypoxia acclimation to increase flux rates during submaximal exercise in highland deer mice. If metabolic regulation changes with acclimation, then we predict that

exercise-induced activation of key proteins in the pathway will also change. Specifically, we predict that PDH activity and sarcolemmal GLUT4 density will be higher at similar submaximal workloads following acclimation to chronic hypoxia. By increasing PDH activity and sarcolemmal GLUT4 content at submaximal workloads, flux rates through the aerobic carbohydrate pathway will be elevated, mirroring the increased carbohydrate oxidation seen at the whole-animal level during submaximal exercise in hypoxia (Lau et al., 2017).

Methods

Experimental Animals

All animal procedures used in this study were approved by the McMaster University Animal Research Ethics Board following guidelines from the Canadian Council on Animal Care. Wild deer mice (*Peromyscus maniculatus*) were trapped at high altitude (HA, 4350 m a.s.l., Mt. Evans, CO) and gastrocnemius muscles sampled at rest or after 20 min of treadmill exercise at approximately 75% VO_2max (Lau et al., 2017). A separate group of wild HA deer mice were trapped and then transferred to McMaster University. These mice were bred to the first laboratory-born generation (G_1) and used for *in situ* muscle stimulation experiments (see below). Mice were housed in common garden conditions (23°C, 12:12 day:night) and fed standard mouse chow (Teklad Global Rodent Diets; Envigo, Mississauga, ON) and water *ad libitum*. Adult G_1 mice were split into 2 acclimation groups: normoxia-acclimated mice remained in common garden conditions, while hypoxia-acclimated mice were placed in hypobaric chambers for 6 weeks (McClelland et al., 1998). These chambers were set to barometric pressures of ~60kPa using a vacuum pump, conditions similar to those found at the summit of Mt. Evans. Mice were removed from hypobaric chambers (~30 min) once per week during the acclimation period for cage cleaning.

In situ Gastrocnemius Stimulation

Mice were fasted for 2-4 hours prior to experimentation to ensure post-absorptiveness: the state where the gastrointestinal tract is clear and nutrient absorption has ceased. By ensuring similar nutritional status between mice, the confounding effects of

nutrient availability on metabolism were controlled. Procedures for dissection and setup of *in situ* stimulation equipment were similar to previous protocols (MacIntosh et al., 2011; Wilson et al., 1967), with modifications. Using an isoflurane vaporizer, general anaesthesia was induced with 100% O_2 at flow rates of 1L/min supplemented with 3% isofluorane. Anaesthesia was confirmed by inability of the animal to right itself and the loss of the toe pinch withdrawal reflex. Isofluorane was then decreased to 2%. The musculature of the upper and lower right hindlimb was exposed and incisions were made in the hindlimb musculature to expose the sciatic nerve, which was then severed rostrally to prevent input from the central nervous system. An incision was made between the Achilles tendon and tibia, followed by the tying of 6-0 suture around the Achilles tendon. The Achilles tendon was then severed below the suture and the gastrocnemius was gently pulled away from the hindlimb and the soleus muscle was then removed. The mouse was transferred to a pad warmed to 37°C as part of an *in situ* mouse apparatus (Aurora 809C; Aurora, ON) and isofluorane vaporization was further reduced to 1-1.5%. The suture tied to the gastrocnemius was secured to the lever arm of a force transducer (Aurora 305C). The right leg was immobilized by taping down the foot and clamping down the knee. Two electrodes attached to a bi-phase stimulator (Aurora 701C) were positioned on opposite sides of the exposed sciatic nerve stump innervating the gastrocnemius. These electrodes delivered bi-phase electrical pulses (see below) set to a constant current of ~560mA using voltages between 0 and ±80V to the sciatic nerve, inducing isometric contractions in the gastrocnemius, which were recorded by the force transducer.

Optimal Length

The gastrocnemius was first stretched to optimal length (L_o), the length at which an electrical stimulus elicited the highest force production during a single twitch (MacIntosh et al., 2011), to control for differences in contractile properties with muscle length (Rassier and MacIntosh, 2002). Force production of individual twitches was measured following application of an electrical stimulus (1ms pulse), which were separated by at least 30 seconds to minimize muscle fatigue. Gastrocnemius length was adjusted by sliding the force transducer or by changing the angle of the lever arm for coarse and fine adjustment, respectively. Moving the force transducer or lever arm away from the mouse stretched the muscle and *vice versa*. L_o was confirmed as the muscle length that generated the greatest difference between resting tension and peak tension during a twitch. L_o was then carefully determined using a pair of calipers (Table A.1).

Muscle Stimulation

Maximal force production (F_{max}) was measured using a series of electric stimuli (0.2ms pulse width, 0.3s duration) applied to the sciatic nerve with increasing frequency of stimulation separated by 2 minutes of rest to limit fatigue. Preliminary experiments measured force production from stimuli of 0 to 200Hz and identified 200Hz as a reliable frequency to elicit F_{max} (Fig. A.1), which was identified as the maximal difference between resting and peak tension in a contraction showing fused tetanus. The F_{max} measurement was performed at least 6 times per mouse to account for contractions that did not show tetanus. Force production from these contractions were averaged to determine F_{max}. Following F_{max}

measurement, the gastrocnemius was stimulated at a light or heavy workload, corresponding to 25 and 50% of F_{max}, respectively. The gastrocnemius was stimulated (0.2s delay, 0.2ms pulse width, 0.2s duration) 3-5 times at multiple frequencies between 30-80Hz. The frequency that elicited force production closest to 25% or 50% of F_{max} was then applied as a train at a frequency of 0.2 trains per second over 3 min, similar to methods used by previous studies that induced PDH activation in an *in vitro* model (Herbst et al., 2012). Immediately following the final contraction, the mouse was quickly removed from the set up, euthanized via cervical dislocation and the stimulated gastrocnemius was quickly removed and freeze-clamped using aluminum tongs cooled in liquid N_2, with the contralateral gastrocnemius frozen as a resting control (Wilson et al., 1967).

PDH Assay

PDH activity (PDHa) and total PDH activity (PDHt) were measured in crude muscle homogenates as previously described (Constantin-Teodosiu et al., 1991) with modifications (Putman et al., 1993). Frozen gastrocnemius samples (5-10mg wet weight) were first diluted 30x in homogenization buffer on ice for PDHa (in mM): sucrose 200, KCl 50, $MgCl_2$ 5, EGTA 5, Tris HCl 50, NaF 50, DTT 1, DCA 1; 0.1% (v/v) Triton X-100; pH 7.8) and for PDHt (in mM): sucrose 200, KCl 50, $MgCl_2$ 5, EGTA 5, Tris HCl 50, glucose 10, $CaCl_2$ 10, DTT 1, DCA 10, Hexokinase 2 U/mL, Triton X-100 0.1% (v/v); pH 7.8). Samples were then homogenized using manual glass-on-glass homogenizer followed by mechanical (400rpm) Teflon-on-glass homogenization on ice for 30s each. To limit vesicle formation that masks PDH activity, homogenates were quickly snap-frozen in liquid nitrogen and stored at -80°C until further analysis.

PDH Reaction

Homogenates were thawed and vortexed immediately before use and were used in less than 2 days from initial freezing. Aliquots of 30µL of homogenate were added to 720µL of PDH reaction mixture containing (in mM) PDH assay buffer: 108.3 Tris, 0.54 EDTA, 1.08 $MgCl_2$, pH 7.8, with 3 NAD, 1 CoASH, and 1 TPP. Each sample was measured in duplicate with a blank at 37°C using a dry block heater (Fisher Scientific; Ottawa, ON). The PDH reaction was initiated with the addition 30 µl of 26mM pyruvate in duplicate and dH_2O for the blank. Reaction mixtures were mixed at the beginning of the reaction via gentle vortexing and throughout the reaction via pipetting to minimize time spent out of the dry block heater. At precisely 1-, 2- and 3-minute time points after adding pyruvate or dH_2O, 200µL of the PDH mixture was removed and added to 40µL of 0.5N $HClO_4$. Following the completion of all reactions, the acidified mixtures were placed on ice for at least 5 min to ensure reactions were halted and then samples were neutralized (pH ~6.5) with the addition of 12-14µL of fresh 1M K_2CO_3. These samples were left to sit for at least 5 min at room temperature before being stored at -80°C until further analysis.

Acetyl-CoA Determination

PDH activity was determined by measuring acetyl-CoA formation over time using radiolabelled oxaloacetate as substrate, as described previously (Cederblad et al., 1990; Cooper et al., 1986) with modifications (Constantin-Teodosiu et al., 1991). ^{14}C-oxaloacetate was prepared via transamination of ^{14}C-aspartic acid (Equation 2), as previously described (Siess et al., 1976) with modifications (Cooper et al., 1986). ^{14}C-

oxaloacetate formation was performed concurrently with the acetyl-CoA assay to limit spontaneous decomposition to pyruvate. In an Eppendorf tube, 9µL of ^{14}C-aspartic acid (Perkin Elmer L-^{14}C(U)-Aspartic acid; 0.1µCi/µL), 5µL of 80mM α-ketoglutarate (prepared fresh), 50µL of 7mM EDTA, 20µL of 500mM HEPES (pH 7.4), 86µL of dH_2O and 10µL of 100U/mL glutamate oxaloacetic transferase (GOT; aka aspartate aminotransferase) were combined and incubated at room temperature for 10 minutes. The transamination reaction was stopped with the addition of 10µL of 1M $HClO_4$ and left on ice for 10 minutes. The solution was then neutralized with 360µL of 11mM EDTA (pH 7.4) and 40µL of 600mM KOH, then left on ice for at least 5 minutes prior to use. ^{14}C-oxaloacetate was used in less than 1 hour after formation.

Reaction products collected from the PDH reaction (see above) were thawed and spun at 10,000g for 3 min to pellet the insoluble fraction, consisting of cellular debris and $KClO_4$. Then 5-40µL of the supernatant was diluted with dH_2O to 200µL. Samples were assayed within 1 week of initial freezing and within 2 freeze-thaw cycles. Next, 2µL of 100mM DTT and 20µL of $CuSO_4$-K^+-acetate (3/2/2 v/v/v 1mM $CuSO_4$, 400mM K^+-acetate, dH_2O) were added to each sample and vortexed. Samples were then incubated at room temperature for 30 min, to remove endogenous oxaloacetate and citrate, thereby limiting endogenous acetyl-CoA formation (Cooper et al., 1986). Roughly halfway through this incubation step, formation of the labelled ^{14}C-oxaloacetate was initiated (see above). After the 30min room temperature incubation, samples were placed on ice for 10 min. Then, 20µL of 60mM EDTA were added and after 5 min at room temperature, 30µL of 30mM NEM was added, followed by incubation at room temperature for 5 min to remove excess

CoASH. To convert acetyl-CoA to ^{14}C-citrate, 10µL of 220 U/mL citrate synthase and 20µL of ^{14}C-oxaloacetate were added to each sample, vortexed and incubated at room temperature for 20min (Reaction 1). To convert excess unmetabolized ^{14}C-oxaloacetate to ^{14}C-aspartate, 10µL of 100 U/mL GOT and 20µL of 275mM glutamate were added to each sample, mixed and incubated at room temperature for 20min (Equation 2). The excess ^{14}C-aspartate containing negatively charged amine groups was then removed with the addition of 1mL of 37.5% (w/v) Dowex cation exchange resin slurry (5OW-X8 H^+ form, 100-200 mesh) and mixed manually via inversion for 2 min. Samples were spun at 1200 g for 5 min at room temperature to sediment the resin. 500µL of supernatant was removed from each sample and added to 5mL of scintillation cocktail (EcoScint A; National Diagnostics, Atlanta, GA) in 20mL scintillation vials (Wheaton; Millville, NJ). The ^{14}C-citrate was quantified using liquid scintillation counting (Perkin-Elmer; Waltham, MA) and acetyl-CoA concentrations were calculated using a standard curve for each ^{14}C-oxaloacetate preparation (Fig. 1).

$$Acetyl\text{-}CoA + {}^{14}C\text{-}Oxaloacetate \xrightarrow{CS} {}^{14}C\text{-}Citrate + CoASH \quad (1)$$

$$^{14}C\text{-}Aspartate + \alpha\text{-}ketoglutarate \xleftrightarrow{GOT} {}^{14}C\text{-}Oxaloacetate + Glutamate \quad (2)$$

Calculation of PDH Activity Values

PDH activity was calculated as the formation of acetyl-CoA over time, standardized to muscle wet weight. The counts per minute (CPM) values obtained from liquid scintillation counting were converted to acetyl-CoA concentrations using a standard curve

(Fig. A.2). Rates of acetyl-CoA formation over time were determined by averaging the slopes of the linear regressions for the technical replicates and subtracting the slope of the blank lacking substrate. This activity value was then multiplied by a dilution factor to standardize for tissue wet weight (Table A.2).

Subcellular Fractionation

Samples were prepared as described previously (Dubouchaud et al., 2000; McClelland and Brooks, 2002; Templeman et al., 2012) with modifications. 50-75mg of frozen gastrocnemius tissue was diluted 5x (w/v) in Buffer A (in mM: 210 sucrose, 2 EGTA, 40 NaCl, 30 HEPES, pH 7.4, 0.75% protease inhibitor cocktail) and homogenized on ice at 400 rpm for 30 seconds using a Teflon pestle in a glass mortar. This crude homogenate was then centrifuged at 600g for 10 min at 4°C. The pellet was discarded, and the supernatant was further centrifuged at 10,000g for 20 min at 4°C for isolation of the sarcolemmal fraction (SL). The resulting supernatant was diluted with 0.75 x volume of Buffer B (1.167M KCl, 58.3mM Na_4PPi, pH 7.4) and spun at 232,000g for 2 hours at 4°C. The supernatant was discarded, and the pellet was washed with Buffer C (10mM Tris, 1mM EDTA, pH 7.4) to limit cross-fraction contamination, and then re-suspended in 24µL of Buffer C with 8µL of 16% SDS. This suspension was spun at 10,000g for 25 min at 25°C. The resulting supernatant was collected as the SL fraction. Protein concentration was determined with bicinchoninic acid assay (Smith et al., 1985) using bovine serum albumin as a standard. Samples were stored at -80°C until further analysis.

Western Blotting

Sarcolemmal GLUT4 was measured via SDS-PAGE and immunoblotting of the SL fractions (Towbin et al., 1979). Membrane fraction samples were diluted with H_2O and Laemmli buffer to 0.5µg/µL and denatured at 95°C for 5 minutes. 20 µL of sample were then loaded to each well in a hand-casted gel consisting of 4% polyacrylamide stacking gel above a 12% resolving gel (Bio-Rad, Mississauga, ON). The gel was then bathed in Tris/glycine running buffer (25mM Tris, 192mM glycine, 0.1% SDS) that contributed to denaturation of the sample proteins and allowing current to move through the gel. Proteins were separated using a voltage of 100V for 15 min, followed by 150V for 60 min. Once voltage was removed, gels were cut at the dye front and edge of the resolving gel, then removed and placed in transfer buffer (running buffer + 10% methanol) to equilibrate for 30 min to 1 hour. A piece of polyvinylidene fluoride (PVDF) membrane was cut to fit the gel and soaked in 100% methanol for 2 min. A sandwich consisting of membrane pads and filter paper soaked in transfer buffer, gel and PVDF membrane was assembled and clamped. The sandwich was bathed in chilled (4°C) transfer buffer and a voltage of 100V was applied for 90 min, using a Bio-Rad Mini-Protean System. Temperature and ion concentrations were maintained using pre-chilled freezer pack, ambient cold (4°C) and constant stirring. Following voltage removal, blots were left in blocking buffer (5% (w/v) fat-free milk (Carnation; Markham, ON) in 0.1% TWEEN phosphate-buffered saline (PBS-T)) overnight at 4°C. Complete protein transfer from the gel was verified by the absence of bands on gels following 1 hour of staining with Coomassie Brilliant Blue and 1 hour of destaining in H_2O.

Blots were incubated in primary GLUT4 antibody (Abcam 33870; poly-clonal, rabbit), diluted 1:1000 (1µg/mL) in 1% (w/v) BSA PBS-T for 1 hour at room temperature. Blots were then rinsed with PBS-T in the following order: 3 quick rinses, one 15 min rinse and 3 consecutive 5 min rinses. Blots were then incubated with anti-rabbit secondary antibody diluted to 1:10000 in 1% BSA PBS-T for 1 hour at room temperature. Blots were then rinsed with PBS-T as described above. Following the PBS-T rinses, blots were incubated with 1mL of H_2O_2 Bio-Rad Clarity substrate for 2 min. Blots were imaged using chemiluminescence on a Bio-Rad ChemiDoc; images were chosen based on exposure time that produced the darkest bands without reaching saturation. Total protein loaded was then measured using Coomassie staining. First, blots were rinsed with dH_2O, then stained with Coomassie dye for 5 min. After, blots were de-stained with 3 washes for 3 min of 50% methanol + 1% acetic acid, followed by 3 min of 10% methanol. Blots were dried and bands were imaged using a ChemiDoc to quantify total protein. GLUT4 band intensity was standardized to total protein intensity and then standardized to the signal of a common sample loaded between gels as an inter-gel control.

Metabolite Assays

Frozen gastrocnemius was homogenized in 6% $HClO_4$ on ice, then spun at 10,000g for 10 minutes at 4°C. The supernatant was taken and then neutralized with 3M K_2CO_3. The homogenate was spun again (as above) and the supernatant was taken. The following metabolites were assayed in duplicate with a spectrophotometer by placing sample in buffer and measuring absorbance (340nm) before and after addition of a coupling enzyme. ATP: sample added to buffer (in mM: 5 glucose, 2 NADP, 5 $MgCl_2$, 1 U/mL G6PDH, 20 Tris

(pH 8)) and absorbance was measured before and after a 20 minute incubation at 37°C with the addition of hexokinase (HK; 1.5U/well). CrP: measured in the same wells used for ATP assays. First, 2uL of 1mM ADP were added per well, then absorbance was measured before and after a 25 minute incubation at 37°C with addition of 12.5 U of creatine phosphokinase. ADP: sample added to buffer (in mM: 5 PEP, 0.15 NADH, 5 $MgCl_2$, 500 TEA (pH 7.4), 2.75 U/mL LDH). Absorbance was measured before and after a 25 minute incubation at 37°C with addition of pyruvate kinase (PK; 1U/well). Cr: measured in the same wells used for ADP assays. ATP was added to each well (5mM) and absorbance was measured before and after 37°C incubation for 25 minutes with addition of creatine phosphokinase (12.5U). Pyruvate: sample added to buffer (in mM: 0.15 NADH, 500 TEA, 5 EDTA). Absorbance was measured before and after a 30 minute incubation at 37°C with addition of lactate dehydrogenase (LDH; 1U/well). Lactate: sample added to buffer (glycine, 2.56mM NAD) and absorbance was measured before and after incubation with LDH for 30 minutes at 37°C.

Enzyme Assays

The apparent Vmax of multiple enzymes was assayed *in vitro* by measuring changes in absorbance proportional to enzyme activity. 5-10mg of frozen gastrocnemius was homogenized on ice in buffer (in mM: 100 KH_2PO_4, 5 EDTA, 0.1% v/v Triton-X 100) using a glass mortar and pestle and diluted to 20x. Measurements were performed in triplicate with one blank lacking substrate to measure background activity. Assay conditions were as follows (in mM): LDH 0.28 NADH, 40 Tris (pH 7.4), ± 1 pyruvate; CS

40 Tris (pH 8.0), 0.1 DTNB, 0.22 acetyl-CoA, ± 0.5 oxaloacetate; PK 50 imidazole, 5 ADP, 100 KCl, 10 $MgCl_2$, 0.15 NADH, 10 fructose-1,-6-P, 9.25U/well LDH, ± 5 PEP; HOAD 100 TEA-HCl (pH 7.0), 0.15 NADH, ± 0.1 acetoacetyl-CoA; MDH 100 KH_2PO_4 (pH 7.4), 0.15 NADH, ± 0.5 oxaloacetate. Assays were performed at 37°C in 96-well plates. Absorbance was measured with a spectrophotometer for 5 minutes at 340nm for all assays except CS, which was assayed at 412nm.

Statistical Analyses

Data was analyzed with SigmaStat 3.5 (Systat Software Inc.; San Jose, CA) for significant differences ($p<0.05$) using either a 1-way or 2-way analysis of variance (ANOVA), with Holm-Sidak *post hoc* testing to determine individual differences. Resting metabolite data were analyzed using Student's T-test.

Results

Total PDH Activity

Total muscle PDH activity (PDHt) was significantly different between groups ($F=8.911$, $p<0.001$). PDHt was not different between acclimations in the G_1 mice but was significantly higher in the wild mice than normoxia ($p=0.003$) and hypoxia ($p=0.0003$) acclimated G_1 mice (Fig. 2.1).

Resting PDHa Activity

PDHa activity was significantly different between groups ($F=10.872$, $p = 0.001$). Resting PDHa was not different between acclimations in the G_1 mice but was higher in wild mice than normoxia ($p=0.0003$) and hypoxia (0.0022) acclimated G_1 mice (Fig. 2.2).

Exercised PDH Activity

PDHa activity in the stimulated gastrocnemius was different between groups, as there was a significant interaction effect between workload and acclimation ($F = 7.707$, $p = 0.014$; Fig. 2.3). PDHa activity was significantly higher in hypoxia-acclimated G_1 mice than in normoxia-acclimated G_1 mice, but only at the light workload ($p = 0.025$). While the normoxic mice significantly increased PDHa activity from light to heavy workload ($p = 0.037$), there was no significant workload effect in the hypoxia-acclimated mice (Fig. 2.3). As a result, PDH activity converged at the heavy workload resulting in no differences in activity between the acclimation groups (Fig. 2.3). We also measured PDHa in the gastrocnemius of wild HA mice at rest or immediately post submaximal running (Fig. 2.4). No differences were found between resting and post-running PDHa ($t_{10} = 1.217$, $p = 0.252$).

Sarcolemmal GLUT4 Protein

To determine if hypoxia acclimation led to changes in membrane permeability to glucose, we assessed GLUT 4 in sarcolemmal cell fractions after stimulation. We found no significant effects of acclimation or workload on sarcolemmal GLUT4 protein content (Fig. 2.5). Similarly, sarcolemmal GLUT4 protein content was not different between acclimations in the resting gastrocnemius (Fig. 2.6).

Gastrocnemius Metabolites

To further understand the cellular conditions during muscle contraction we assessed levels of some key metabolites (Table 2.1). There were no significant differences between any groups for concentrations ATP, Cr, pyruvate or any of the metabolite ratios. However, significant interaction effects between acclimation and workload were found for ADP ($p=0.038$), CrP ($p=0.009$) and lactate ($p=0.023$). Hypoxic mice had higher ADP ($p=0.04$) and lower lactate ($p=0.02$) concentrations than normoxic mice, respectively. CrP was the only metabolite with a significant effect of workload within an acclimation; in normoxia acclimated mice, CrP was higher ($p=0.013$) with heavy workload. Within the light workload, CrP was higher in hypoxia-acclimated mice compared to normoxic mice ($p=0.006$). In the light workload, lactate was lower ($p=0.064$) and ADP was higher ($p=0.060$) in hypoxia-acclimated compared to normoxic acclimated G_1 HA deer mice.

The same metabolites were also measured in resting gastrocnemius of the G_1 mice (Table 2.2). There were no significant differences between acclimations for ADP, lactate, pyruvate or any of the metabolite ratios. ATP ($t_{12} = -2.862$, $p =0.014$), CrP ($t_{12} = -3.779$, p

= 0.003) and Cr (t_{11} = -2.890, p = 0.015) were significantly higher in the hypoxia-acclimated mice. While not a significant difference, pyruvate concentration in normoxia-acclimated mice was trending toward higher than hypoxia-acclimated mice (t_{13} = 2.000, p = 0.067).

Enzyme Assays

We measured the maximal activity (V_{max}) of 5 enzymes involved in various pathways of fuel metabolism in the gastrocnemius to investigate differences in capacities for pathway flux between acclimation groups and wild highland deer mice (Table 2.3). The absolute activity of most enzymes (HOAD, PK, CS, LDH) was not different between the groups, apart from MDH (F=4.738, p = 0.020), which was higher in the wild mice than the hypoxia acclimated G_1 mice (p=0.006). Similar trends were found for the enzyme activity ratios: no differences were found in most ratios measured (LDH/CS, LDH/HOAD, PK/LDH, MDH/LDH), but HOAD/CS was different between groups (F = 3.610, p = 0.045). No significant differences between individual groups were identified, but wild mice trended toward higher HOAD/CS compared to G_1 mice acclimated to normoxia (p = 0.031, α = 0.975) and hypoxia (p = 0.029, α = 0.983).

Figure 2.1. Total pyruvate dehydrogenase (PDHt) activity in gastrocnemius of wild deer mice sampled at HA and G_1 deer mice acclimated to normoxia or chronic hypobaric hypoxia. PDH activity standardized to tissue wet weight. PDH activity measured in single leg or averaged across both legs of an individual mouse. Data presented as mean ± SEM. N = 9-12. Bars that do not share a letter are significantly different ($p<0.05$), using 1-way ANOVA and Holm-Sidak *post hoc* testing.

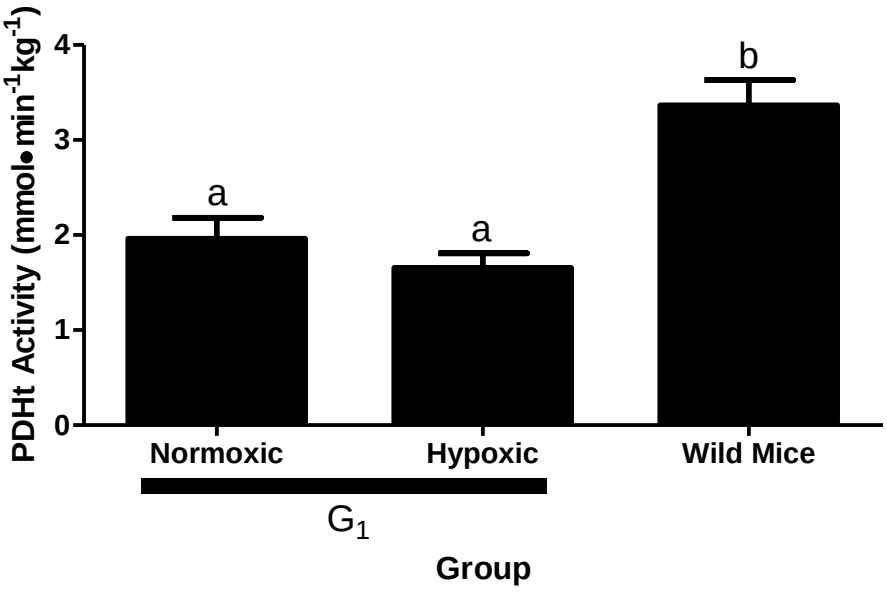
PDHt Activity (mmol• min-1kg-1)
4
3
2
1
0
a
a
b
Normoxic
Hypoxic
Wild Mice
G1
Group

Figure 2.2: Pyruvate dehydrogenase (PDHa) activity in resting gastrocnemius muscle of wild highland deer mice sampled at high altitude and G_1 mice acclimated to normoxia or chronic hypobaric hypoxia, sampled under acute normoxia. PDH activity standardized to tissue wet weight. Data presented as mean ± SEM. N = 4-9. Bars that do not share letters signify significant differences ($p<0.05$) using 1-way ANOVA and Holm-Sidak *post hoc* testing.

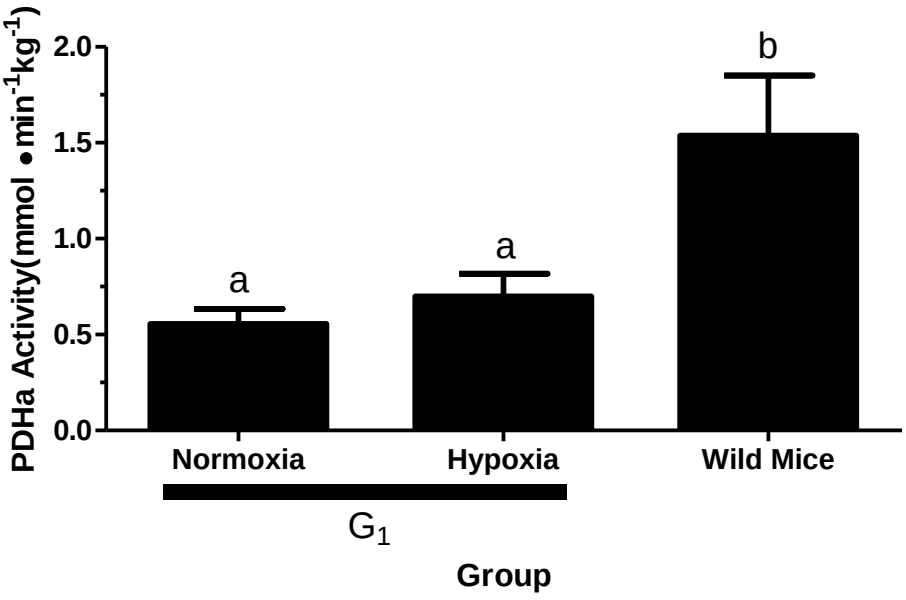
PDHa Activity(mmol • min-1kg-1)
2.0
1.5
1.0
0.5
0.0
a
a
b
Normoxia
Hypoxia
Wild Mice
G1
Group

Figure 2.3. Pyruvate dehydrogenase (PDHa) activity in G_1 highland deer mouse gastrocnemius *in situ* preparation with stimulation. Empty bars represent normoxia-acclimated deer mice; filled bars represent hypoxia-acclimated deer mice. Light workload are muscles stimulated at 25% maximum force (F_{max}); Heavy workload represents muscles stimulated at 50% F_{max}. PDHa activity was standardized to muscle wet weight. Data presented as mean ± SEM. N = 3. †represents significant ($p<0.05$) acclimation effect within a workload; *represents significant ($p<0.05$) exercise effect within an acclimation (2-way ANOVA; Holm-Sidak post-hoc test).

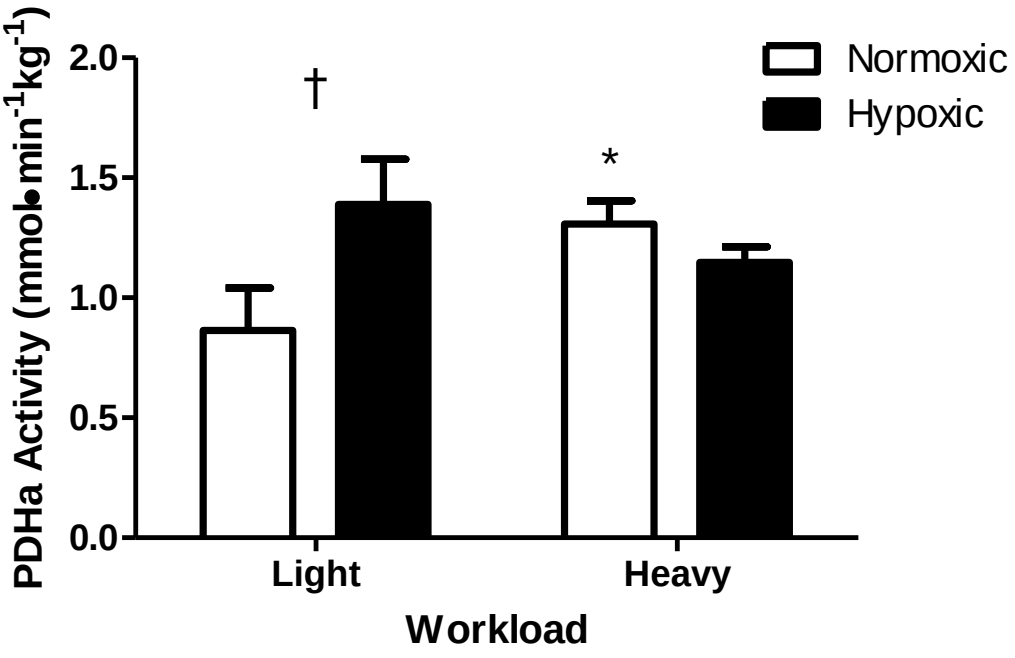
PDHa Activity (mmol•min-1kg-1)
2.0
1.5
1.0
0.5
0.0
†
*
Normoxic
Hypoxic
Light
Heavy
Workload

Figure 2.4. Pyruvate dehydrogenase (PDHa) activity in wild deer mouse gastrocnemius sampled at rest or post-submaximal running at 75% VO_2max sampled at high altitude. PDHa activity was standardized to muscle wet weight. Data presented as mean ± SEM. N = 4-8.

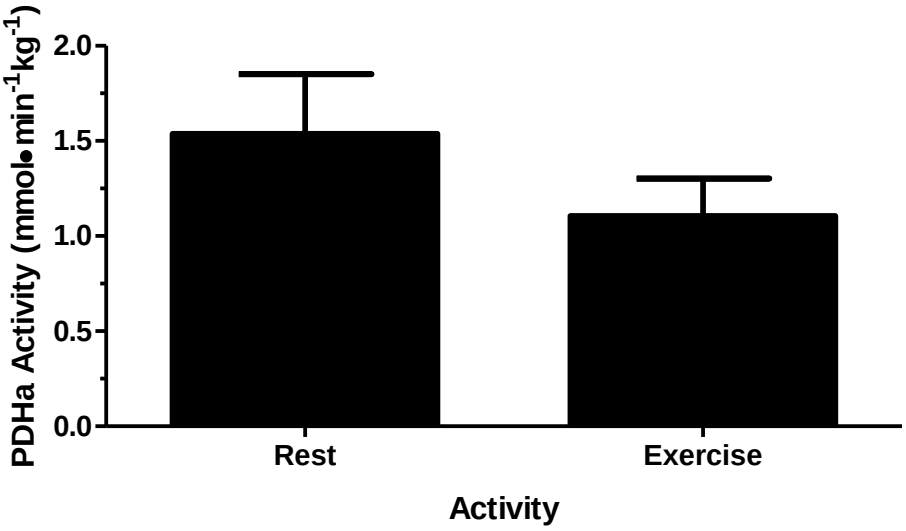
PDHa Activity (mmol• min-1kg-1)
2.0
1.5
1.0
0.5
0.0
Rest
Exercise
Activity

Figure 2.5. Glucose transporter (GLUT)4 protein content from gastrocnemius sarcolemmal fractions of stimulated *in situ* preparations from G_1 highland deer mice. GLUT4 band volume standardized to total lane protein and to an inter-gel standard sample. Light workload mice stimulated at 25% F_{max}; Heavy workload mice stimulated at 50% F_{max}. Empty bars represent normoxia-acclimated mice, filled bars represent hypoxia-acclimated mice. Representative blots presented above data. Data presented as mean ± SEM. N = 3-6.

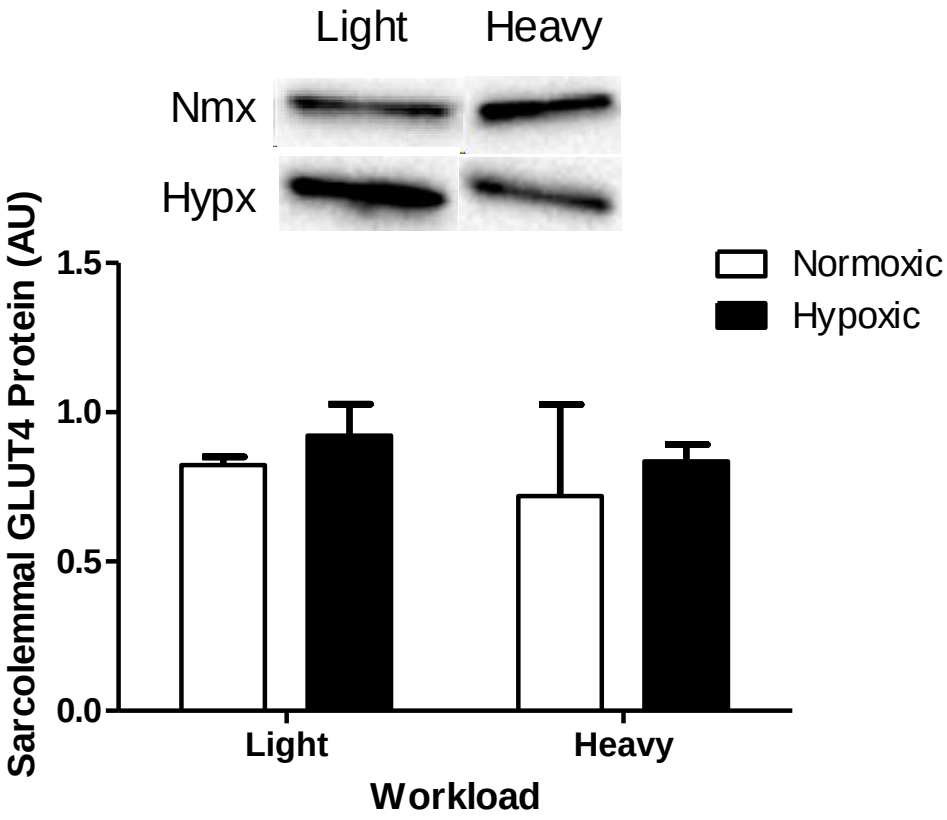
Light
Heavy
Nmx
Hypx
Normoxic
Hypoxic
Sarcolemmal GLUT4 Protein (AU)
1.5
1.0
0.5
0.0
Light
Heavy
Workload

Figure 2.6. Glucose transporter (GLUT)4 protein content from sarcolemmal fractions of resting gastrocnemius from G_1 highland deer mice. GLUT4 band volume standardized to total lane protein and to an inter-gel standard sample. Representative blots presented above data. Data presented as mean ± SEM. N = 2-6.

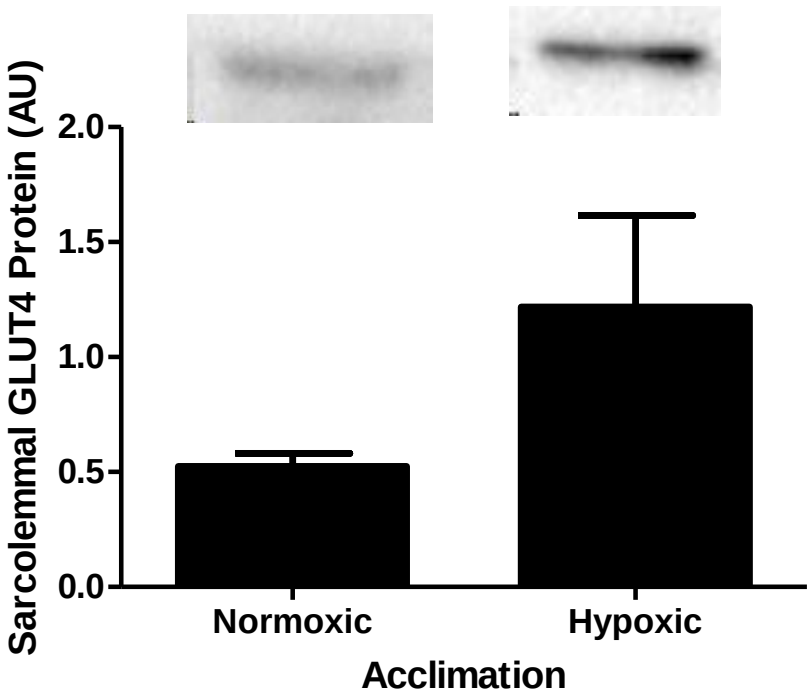
Sarcolemmal GLUT4 Protein (AU)
2.0
1.5
1.0
0.5
0.0
Normoxic
Hypoxic
Acclimation

Table 2.1. Metabolites in stimulated gastrocnemius of G_1 deer mice. Data presented as mean ± SEM. All values are µmol/g wet weight. Cr: free creatine; CrP: creatine phosphate. Significant ($p<0.05$) differences signified by # main interaction effect; * main acclimation effect; † workload effect within acclimation; $ acclimation effect within workload. ($) signifies acclimation effect approaching significance ($p<0.07$). 2-way ANOVA with Holm-Sidak *post hoc* analysis. N = 3-5.

	Normoxia		Hypoxia	
	Light	Heavy	Light	Heavy
ATP	3.56 ± 0.72	4.39 ± 0.84	5.52 ± 0.65	4.94 ± 0.72
ADP # *	1.90 ± 0.17	2.78 ± 0.53	3.85 ± 0.81 ($)	4.06 ± 1.06
CrP #	7.02 ± 0.70	10.98 ± 0.98 †	11.52 ± 1.03 $	9.26 ± 1.17
Cr	4.72 ± 0.29	7.92 ± 2.05	7.77 ± 2.90	15.84 ± 6.92
Pyruvate	2.85 ± 0.30	2.60 ± 0.40	3.83 ± 0.87	3.13 ± 0.13
Lactate # *	3.62 ± 0.44 ($)	3.63 ± 0.85	1.81 ± 0.29	2.14 ± 0.60
ATP/ADP	1.67 ± 0.35	2.48 ± 0.62	1.75 ± 0.45	1.48 ± 0.52
CrP/Cr	1.18 ± 0.17	1.98 ± 0.69	2.45 ± 0.68	1.53 ± 1.14
CrP/ATP	3.20 ± 0.96	2.22 ± 0.45	2.13 ± 0.12	1.94 ± 0.35

Table 2.2. Metabolites in resting gastrocnemius of first generation (G_1) laboratory born and raised deer mice. Data presented as mean ± SEM. All values are µmol/g wet weight. Cr: free creatine; CrP: creatine phosphate. Significant ($p<0.05$) differences denoted by *. Differences approaching significance ($p<0.07$) denoted by (*). Student's T-test. N = 7-9.

	Normoxia	Hypoxia
ATP *	4.36 ± 0.37	6.75 ± 0.75
ADP	2.97 ± 0.63	2.66 ± 0.33
CrP *	6.68 ± 0.78	9.97 ± 0.38
Cr *	4.43 ± 0.57	9.28 ± 1.47
Pyruvate (*)	3.15 ± 0.25	2.30 ± 0.33
Lactate	4.62 ± 0.91	4.76 ± 0.81
ATP/ADP	2.11 ± 0.61	2.71 ± 0.42
CrP/Cr	1.53 ± 0.38	1.04 ± 0.16
CrP/ATP	1.52 ± 0.09	1.36 ± 0.24

Table 2.3. Enzyme activities and ratios in gastrocnemius of highland deer mice. Enzyme activity reported in µmol/min/g wet weight. Data presented as mean ± SEM. N = 8. * indicates significant difference within an enzyme and different letters signify significant difference between groups in an enzyme. 1-way ANOVA with Holm-Sidak *post hoc* testing.

	Normoxic G_1	Hypoxic G_1	Wild
HOAD	29.5 ± 3.0	24.6 ± 3.3	34.0 ± 2.12
MDH *	692 ± 55[a]	540 ± 27[a]	904 ± 132[b]
PK	181 ± 17	154 ± 8	170. ± 8
CS	40.6 ± 3.1	34.6 ± 2.0	35.6 ± 4.1
LDH	280 ± 21	271 ± 11	299 ± 14
HOAD/CS *	0.73 ± 0.06	0.73 ± 0.10	1.02 ± 0.10
LDH/CS	7.13 ± 0.70	7.97 ± 0.43	8.99 ± 0.96
LDH/HOAD	9.87 ± 0.84	12.57 ± 1.90	9.01 ± 0.69
PK/LDH	0.64 ± 0.03	0.58 ± 0.04	0.57 ± 0.03
MDH/LDH	2.54 ± 0.23	2.03 ± 0.15	3.08 ± 0.46

Discussion

The aim of this study was to investigate changes in the metabolic regulation of the CHO pathway in deer mouse gastrocnemius after acclimation to chronic hypoxia. By investigating changes in metabolic regulation, we sought to establish a mechanistic explanation for changes in fuel use during submaximal exercise at the whole-animal level. We found higher PDH activation and lower lactate concentrations in gastrocnemius of hypoxia-acclimated mice than normoxia-acclimated mice at similar submaximal workloads. Conversely, we found no differences in sarcolemmal GLUT4 density or maximal activity of multiple enzymes with acclimation in the G1 mice. These data support our hypothesis by indicating changes in metabolic regulation of the CHO pathway with hypoxia acclimation but suggest that that such changes are not consistent between steps of the CHO pathway. By elevating PDH activity and decreasing lactate accumulation, hypoxia-acclimated G_1 mice are able to support higher flux rates through the CHO pathway, thereby supporting higher rates of CHO at the whole-animal level under submaximal intensities.

This study is the first to our knowledge to investigate changes in metabolic regulation of the carbohydrate oxidative pathway in mice using an *in situ* muscle stimulation approach. Benefits of using an *in situ* approach include having a fine level of control over muscle workload, preservation of physiological conditions and shortened sampling times post-contraction, which are critical for accurately capturing the exercise metabolic phenotype. Similar studies have been performed using *in vitro* muscle stimulation (e.g., Dunford et al., 2011; Herbst et al., 2012), but the size of the deer mouse gastrocnemius is

too large for such an approach due to limitations in O_2 delivery (Segal and Faulkner, 1985). In contrast, O_2 and substrate delivery are not limiting for *in situ* approaches due to an intact circulation to the gastrocnemius (McDonald et al., 1992).

A weakness of this study is the inherent difficulty in comparing workloads of an isolated muscle to workloads at the whole-animal level. Not only is there a large difference between modes of exercise in the number of levels of physiological organization involved, the metrics used to measure workload are distinct. Typically, isolated muscle workloads are measured as force production, while whole-animal workloads are measured as O_2 consumption rates. While force production measures energetic output that may be supplied by aerobic and anaerobic metabolism, O_2 consumption rates reflect energetic output supplied only by aerobic metabolism. It is for these reasons that direct comparisons between modes of exercise should be avoided and instead, comparisons between workloads within each mode of exercise should be made.

PDHt activity did not change with acclimation in the G_1 mice, indicating that the capacity for pyruvate oxidation is unchanged in hypoxia. This finding is in accordance with a previous mitochondrial study from our lab (Mahalingam et al., 2017) that found no differences with hypoxia acclimation in pyruvate-fuelled mitochondrial respiration in permeabilized gastrocnemius fibers. Surprisingly, PDHt activity was significantly higher in gastrocnemius from wild mice than in the G_1 mice. In addition, CS activity was not different between the G_1 and wild mice, indicating that differences in PDHt activity are not the result of changes in mitochondrial volume (Larsen et al., 2012). This suggests that wild deer mice may have an enhanced capacity for aerobic CHO during exercise compared to

G_1 mice and that they do so through mitochondrial remodelling. Differences between G_1 and wild mice phenotype indicate that likely both developmental and adult plasticity have effects on determining whole-animal fuel selection patterns during exercise in the wild. While phenotype appears to converge at the whole-animal level, adult and developmental plasticity may induce different underlying biochemical mechanisms. Specifically, adult plasticity appears to promote elevated PDHa in exercising muscle, while combined with developmental plasticity appears to promote elevated PDHt.

In accordance with our predictions, we found that PDHa activation was higher in hypoxia-acclimated mice than normoxia-acclimated mice under a light workload, and that PDHa activation converges between acclimations at the heavy workload. By supporting higher PDH activity at submaximal workloads, hypoxia-acclimated mice may sustain elevated rates of aerobic CHO in muscle, as was seen in whole-animal fuel selection patterns in deer mice during submaximal exercise (Lau et al., 2017). Since glucose has a relatively high ATP yield per O_2 (Brand, 2005; Welch et al., 2007), increased PDH activity at submaximal exercise should translate to elevated exercise performance in hypoxia.

The primary determinant of PDH activity is phosphorylation state resulting from the relative activity of PDK and PDP (Linn et al., 1969). Therefore, the increased PDH activity following hypoxia acclimation suggests higher rates of PDH dephosphorylation, which may be achieved by increases in PDP activity and/or decreases in PDK activity. Both PDK and PDP are regulated allosterically by cellular energy markers, such as pyruvate and ATP/ADP concentration ratios (Pettit et al., 1975). While there are additional allosteric regulators of PDK and PDP activity not measured in our study (CoASH/acetyl-CoA,

NAD^+/NADH, Ca^{2+}; Denton et al., 1972; Pettit et al., 1975), our metabolite data did not show any changes in gastrocnemius energy status between acclimations, therefore indicating that changes in PDK or PDP activity with acclimation are likely the result of changes in expression.

In muscle, the 4 PDK and 2 PDP isoforms vary in plasticity of expression and regulatory pathways. For example, both PDK2 and PDK4 are responsive to nutrient and hormonal sensors (Sugden and Holness, 2006), which may change during hypoxia exposure and downregulate total PDK expression. To date, only PDK1 expression has been found to be plastic in response to environmental hypoxia exposure. The transcription factor hypoxia-inducible factor (HIF), has been linked to PDK1 expression in cellular (Kim et al., 2006; Papandreou et al., 2006) and rodent (Dunford et al., 2011; Le Moine et al., 2011) models. While PDK1 can phosphorylate the first 2 phosphorylation sites of the α subunit of PDH (Ser^{264}, Ser^{271}), PDK1 is unique among the PDK isoforms by its ability to phosphorylate the third phosphorylation site (Ser^{203}) (Korotchkina and Patel, 2001). This characteristic may explain why small increases in PDK1 expression are sufficient to decrease PDH activity despite large decreases in total PDK activity via PDK2 knockout (Dunford et al., 2011). Since PDK1 expression is sensitive to levels of HIF-1α, changes in PDK1 expression are likely requisite for regulating changes in CHO with acclimation to chronic hypoxia (Le Moine et al., 2011). HIF-1α abundance is directly controlled by the activity of prolyl hydroxylase, which degrades HIF-1α in the presence of O_2 (Bruick and McKnight, 2001). While HIF-1α is elevated in acute hypoxia, HIF-1α decreases to normoxic levels with chronic hypoxia exposure (Le Moine et al., 2011). The decrease in HIF-1α is likely

mediated by cellular ‘desensitization’ to HIF by increased activity and expression of prolyl hydroxylase with chronic hypoxia (Ginouvès et al., 2008). Therefore, the increased PDH activation seen with stimulation after hypoxia acclimation in highland deer mice observed in this study may be the result of decreased PDK1 expression via cellular desensitization to HIF.

Previous work that identified elevated CHO rates in exercising hypoxic highland deer mice found no differences from controls in intramuscular glycogen use with exercise (Lau et al., 2017), suggesting a greater reliance on circulating glucose to fuel locomotion in hypoxia. Surprisingly, we found no differences in sarcolemmal GLUT4 protein abundance with exercise or acclimation, suggesting that GLUT4 density at the light workload is sufficient to maintain high MGU rates. This is partially supported by previous transgenic rodent studies that changed the expression of GLUT4 and/or the enzyme hexokinase II. In these studies neither GLUT4 overexpression nor its partial knock out had any effect on exercise MGU, but partial hexokinase knock out significantly decreased exercise MGU (Fueger et al., 2004a; Fueger et al., 2004c). These studies identified hexokinase activity as the rate-determining step of MGU during exercise, therefore suggesting that increases in sarcolemmal GLUT4 density may not be necessary for increasing MGU rates in exercising muscle. Previously, our lab found that hypoxia acclimation increased hexokinase activity in highland deer mouse gastrocnemius (Lau et al., 2017), suggesting that higher MGU rates during exercise may be achieved via increasing rates of glucose phosphorylation without increasing sarcolemmal GLUT4 density.

In conjunction with elevated PDH activity, hypoxia-acclimated mice also showed lower accumulation of intramuscular lactate in the gastrocnemius, despite little change in pyruvate accumulation. These data suggest that a greater relative fraction of glycolysis-derived pyruvate is oxidized via PDH and not reduced by LDH. Since lactate is a metabolic intermediate that diverts carbon away from the mitochondria, reduced lactate accumulation represents an energetic strategy where ATP formation per mole of glucose is increased. In conjunction with an elevated preference for CHO that maximizes ATP yield per O_2, highland deer mice maximize energetic output during exercise at high altitude by minimizing anaerobic glycolysis. A major caveat to our finding of reduced intramuscular lactate accumulation is that we have not measured lactate efflux into the circulation, which may occur via monocarboxylate transporters (Juel and Halestrap, 1999). However, circulating lactate concentrations in post-running deer mice do not support this explanation, as they were unchanged with acclimation (Lau et al., 2017).

We measured various metabolites to assay the energetic status of the gastrocnemius post-contraction. Surprisingly, we found no differences in any of the metabolite ratios, suggesting no differences in the energetic status of the muscle between workloads and acclimations. We similarly found no differences in ATP concentrations, but this was expected as ATP concentrations *in vivo* are tightly guarded by changes in ADP phosphorylation rates (Hochachka and Matheson, 1992). Interestingly, ADP concentrations were higher in the hypoxia-acclimated mice, which could contribute to elevated CHO flux rates due to allosteric activation of proteins in the CHO pathway, such as phosphofructokinase (PFK) (Denton and Randle, 1966). CrP use was apparently lower in

hypoxia acclimation at the light workload, but both acclimations converge at the heavy workload, with no differences in Cr accumulation throughout. This finding was unexpected, as CrP is typically depleted with heavier workloads to form Cr (Kristensen et al., 2015). However, CrP is typically an ATP source used most prevalently in the opening ~30 seconds of an exercise bout (Hultman and Sjöholm, 1983), before aerobic fuel sources may be fully mobilized and oxidative pathway flux is sufficient to meet ATP demand. Therefore, by the end of a 3-minute stimulation protocol, aerobic pathway flux may be high enough to support ATP demands and (at least partially) regenerate CrP stores. Intriguingly, lactate accumulation was lower in the hypoxia-acclimated mice, despite no changes in pyruvate accumulation. This is surprising, given that lactate formation is reversible and reaches an equilibrium with pyruvate formation, suggesting that lactate formation is limited by substrate availability. Pyruvate may by sequestered by to the mitochondria via mitochondrial pyruvate carrier and PDH (Vacanti et al., 2014), while NADH may be sequestered by the malate aspartate shuttle (Wu et al., 2007). As intermediates in anaerobic pathways, higher CrP and lower lactate accumulation in the hypoxia-acclimated mice suggests a greater reliance on aerobic ATP sources to fuel contractions (Hochachka, 1994). Thus, these provide additional support for increased reliance on aerobic CHO to fuel submaximal exercise in hypoxia.

In addition to changes in metabolic regulation, we investigated changes in hierarchical regulation by measuring the activity of multiple gastrocnemius enzymes involved in fuel metabolism. Unlike previous studies from our lab, we measured the activity of the TCA cycle enzyme, MDH, and directly compared the activities of HOAD, PK, LDH, CS and

MDH between the two acclimation groups of G_1 mice and wild mice. The activities of HOAD, PK, LDH and CS were not different between acclimations in the G_1 mice, in accordance with previous studies from our lab (Lau et al., 2017; Lui et al., 2015), a finding shared by MDH activity. Only MDH activity was higher in the wild mice; activity of the other 4 enzymes was not different between wild and lab mice. To supplement the absolute enzyme activity measurements, we also measured enzyme activity ratios to quantify relative flux capacities for multiple pathways. Of the 5 enzyme activity ratios measured, only HOAD/CS was significantly different between groups, with wild mice trending as higher than G_1 mice in either acclimation ($p = 0.03$). A higher HOAD/CS ratio suggests elevated lipid oxidation capacity relative to aerobic metabolism and is likely to support thermoregulation against low ambient temperatures encountered at high altitude. This ratio is elevated in the wild mice likely due to the cold exposure experienced by these mice through development and adulthood, as the G_1 mice were born and raised in common garden conditions. High PK/LDH and MDH/LDH ratios are hypothesized to support aerobic CHO, by limiting pyruvate and NADH flux toward LDH (Hochachka, 1994) yet highland deer mice can increase CHO at the whole animal level without changing either of these ratios. These data suggest that the capacities for multiple fuel metabolism pathways are relatively fixed and provide that changes in CHO pathway flux with acclimation are not due to changes in hierarchical regulation, but metabolic regulation.

Preferential CHO during submaximal exercise is a metabolic strategy that has only been documented in highland taxa (Lau et al., 2017; Schippers et al., 2012), suggestive of selective pressures for this phenotype. The data collected from this study show that the exercise-induced activation of a major determinant of CHO, PDH, changes with hypoxia acclimation in highland deer mice. These are the first data that form a mechanistic explanation for whole-animal fuel selection patterns at high altitude. Subsequent studies should identify causative factors that explain differences in PDH activation during exercise. Changes in PDK1 expression via HIF-1α may be a promising start. In addition, the measurements performed in this study should be repeated in gastrocnemius sampled in G_1 mice immediately post-running at a constant submaximal intensity, to verify that trends seen in a muscle stimulated in isolation match those from an animal engaged in whole-body exercise in the wild. High altitude-native taxa have evolved a metabolic phenotype unique among mammals that deserves further investigation. Such work would be of benefit to the field of comparative physiology, because advancements in the understanding of high altitude bioenergetics would contribute to the understanding of the evolution of phenotypes evolved for high performance in limiting conditions.

CHAPTER 3: Summary and General Discussion

For many years, researchers have been interested in investigating the physiological adaptations used by highland animals to survive at high altitude and how they differ from responses used by lowland natives (Hochachka et al., 1982). The aim of the present study was to provide a mechanistic explanation for the highland deer mouse-specific plasticity in CHO reliance during submaximal exercise (Lau et al., 2017). Past work had suggested that changes in maximum capacities of skeletal muscle glycolytic enzyme could not explain whole animal differences in exercise CHO, indicating that changes in hierarchical regulation are insufficient in explaining the plasticity in whole-animal fuel selection (Lau et al., 2017). Therefore, we examined the role of changes in metabolic regulation as an alternative strategy to promote CHO rates during submaximal exercise. For my thesis, we examined 2 important steps in this pathway known to be regulated in line with CHO in other model systems: GLUT4 translocation for MGU and PDH activation for pyruvate oxidation. We found that hypoxia acclimation does not affect GLUT4 translocation but PDH activity was increased at submaximal workloads in isolated muscle, indicating higher capacity for pyruvate oxidation and thus, CHO. These data provide support for our hypothesis that greater submaximal exercise CHO in highlanders is the result of changes in metabolic regulation of muscle metabolic pathways.

There are long-standing hypotheses regarding high altitude metabolic adaptation that have not been adequately explored. For example, Hochachka (1994) argued that biochemical adaptation to high altitude included 1) maximizing ATP/ mole fuel and 2) maximizing ATP/ mole O_2. Hochachka's first hypothesis is supported by the apparent

preference for CHO at the tissue and whole-animal level in highland natives (Holden et al., 1995; Lau et al., 2017; Schippers et al., 2012) due to a higher ATP yield per O_2 consumed (Brand, 2005; Welch et al., 2007). Hochachka's second hypothesis is supported by the reported prevalence of oxidative muscle phenotypes in some highland natives (Lui et al., 2015; Mahalingam et al., 2017; Scott et al., 2015). A more oxidative phenotype supports elevated rates of O_2 utilization to maintain aerobic metabolism, which produces more ATP per fuel oxidized than via anaerobic metabolism. A classical observation that follows this trend is the 'lactate paradox' (reviewed by Hochachka et al., 2002; Kayser, 1996), where highland natives produce less lactate than lowlanders at similar exercise intensities. Lactate formation represents a potential loss in ATP as ATP produced from lactate is ~5% of the ATP formed from complete glucose oxidation to CO_2.

It presently remains unclear how highland deer mice display appropriate allocation of fuels to different activities of high metabolic demand. Reliance on CHO is upregulated during exercise in hypoxia (Lau et al., 2017) due to high ATP yield per O_2, while lipid oxidation is upregulated during thermogenesis in combined cold and hypoxia (Cheviron et al., 2012; Lyons et al., in prep) due to extensive stores within the body and a high ATP yield per mole fuel. Active muscle is a significant source of energetic output for each activity: active muscle is estimated to be responsible for up to 90% of total O_2 consumption during exercise (Mitchell & Blomqvist, 1971; Weibel et al., 1991) and shivering thermogenesis is responsible for up to 70% of total O_2 consumption during thermogenesis (Nespolo et al., 1999). The primary difference at the whole muscle level between shivering thermogenesis and exercise is the pattern of contractions: coordinated during locomotion

and uncoordinated during shivering. Despite this seemingly simple difference in muscle activation patterns, fuel use is dramatically different between exercise and thermoregulation in the same tissue (Haman and Blondin, 2017).

It is unlikely that highland deer mouse muscle is specialized in the oxidation of either carbohydrates or lipids, as their metabolic pathways are structurally different from each other and can be antagonistic in some circumstances. Instead, deer mice likely increase flux rates at steps shared between each pathway, such as delivery of O_2 and substrate to active muscle and oxidation at the mitochondria. Indeed, capillarity is higher in highland gastrocnemius (Lui et al., 2015; Scott et al., 2015), supporting higher rates of tissue perfusion and promoting increased O_2 extraction (Tate et al., 2017). Further, plasma flow to active tissues may be higher in highland mice in hypoxia due to lower haematocrit (Lui et al., 2015) and similar heart rate (Ivy and Scott, 2017; Lui et al., 2015). At the level of the muscle, total mitochondrial volume is higher in highland deer mice, due to higher volume in the subsarcolemmal subpopulation (Mahalingam et al., 2017). Subsarcolemmal mitochondria are close to capillaries and thus have low diffusion distances for circulating substrates and O_2, thereby greatly increasing accessibility to these resources necessary for aerobic metabolism (Hardy et al., 2009). By increasing the capacity for O_2 and substrate delivery to the mitochondria and their capacity for oxidation, highlanders may have evolved a phenotype optimized for sustaining intensive rates of aerobic metabolism to fuel metabolically demanding activities. While these highland traits help to explain performance differences between populations, many of these traits are unchanged with acclimation as adults in the highland population. Thus, they cannot fully explain the

plasticity in fuel use during exercise or thermoregulation, but the results of the current study indicate that changes in metabolic regulation of fuel metabolic pathways may be contributing to this plasticity.

Future directions

There are other proteins in the muscle CHO pathway that may be sites of additional plasticity in metabolic or hierarchical regulation and represent sites of work that future studies can focus on. Both HK and PFK have high control coefficients in determining glycolytic flux rates (Rapoport et al., 1974), but HK activity is almost entirely controlled by hierarchical regulation, while PFK activity is almost entirely controlled by metabolic regulation (Suarez et al., 2005). This context helps to explain why hypoxia acclimation in highland deer mice increases V_{max} of HK, but not PFK (Lau et al., 2017). The metabolic regulation of PFK would be a worthwhile topic of study, as differences in activity could help to explain trends in glycolytic flux and ultimately pyruvate formation rates for CHO. Glycogen phosphorylase is also a potential site of changes in metabolic regulation with acclimation, but differs from most proteins in that metabolic and hierarchical regulation have roughly equal contributions over regulating flux (Suarez et al., 2005). Intramuscular glycogen use in exercising highland gastrocnemius is similar between normoxia- and hypoxia-acclimated mice, despite large discrepancies in CHO rates (Lau et al., 2017), suggesting an increased reliance on circulating glucose as a intramuscular glycogen-saving strategy. Therefore, glycogen phosphorylase activation may change with acclimation to induce glycogenolysis but only at high workloads. Both PFK and glycogen phosphorylase are subject to allosteric regulation by adenylates and other markers of cellular energy

balance (Cori and Green, 1943; Denton and Randle, 1966), thus acting as a site of activity modulation with acclimation that can be explored with further metabolite studies.

Upstream in the CHO pathway from glucose uptake and oxidation at active muscle is glucose provisioning from the liver. The liver acts as a metabolic hub that finely regulates circulating glucose levels by exporting glucose derived via glycogenolysis and gluconeogenesis (Wasserman, 2008). While blood glucose concentrations are unchanged with exercise in normoxia and hypoxia in highland deer mice, MGU rates are likely elevated to fuel the elevated CHO rates during exercise in hypoxia (Lau et al., 2017). To maintain euglycemia, glucose export by the liver is likely elevated to match MGU rates, suggesting elevated rates of hepatic glycogenolysis and/or gluconeogenesis. However, liver glycogen depletion is similar between groups with a trend for lower depletion after acclimation in HA mice (Lau et al., 2017), suggesting a greater reliance on gluconeogenesis to maintain euglycemia. Differences in hepatic glycogenolytic rates are likely the result of alterations in endocrine signalling from the pancreas via glucagon and adrenal glands via epinephrine (Exton et al., 1972). If muscle phenotype in highland deer mice is adapted to support elevated rates of aerobic CHO, then it is likely that the liver phenotype is similarly adapted to support elevated rates of glucose export to sustain high CHO rates during submaximal exercise.

Implications

Fuel use patterns during exercise are likely to determine behaviours during exercise. By relying on CHO to fuel submaximal exercise, wild highland mice may experience energetic trade-offs in the wild. For example, glucose is stored in relatively limited amounts *in vivo*, and would last up to 25 minutes of exercise at 75% VO_2max (McClelland et al., 2017). By working with such a limited fuel source, mice may shape their behaviour to exercise by relying on short bouts of running to or from shelter to perform ecological activities, such as foraging and mating. This strategy may be beneficial when the consideration of ambient cold is considered. Specifically, time spent outside of shelter is associated with significantly elevated metabolic costs associated with thermogenesis, so minimizing time spent in the cold by quickly running to and from shelter may be adaptive.

The mammalian fuel selection model during exercise has been well characterized and shown to be conserved across a wide range of mammalian taxa (Schippers et al., 2014; Weber and Haman, 2004). Despite such a well-conserved model, highland mice have been observed as exceptions that exhibit an elevated reliance on CHO during submaximal exercise (Lau et al., 2017; Schippers et al., 2012). The underlying mechanisms that allow highland mice to have a high CHO reliance are not well understood, but the findings of this study serve as preliminary evidence indicating that plasticity in metabolic regulation is a contributing factor. It is also unclear if similar degrees of plasticity in metabolic regulation can be found in lowland natives. If lowlanders indeed do not show such plasticity in metabolic regulation, then this plasticity represents a potential trait that allowed highland ancestors to invade the high-altitude niche.

Bibliography

Brand, M. D. (2005). The efficiency and plasticity of mitochondrial energy transduction. *Biochem. Soc. Trans.* **33**, 897–904.

Bruick, R. K. and McKnight, S. L. (2001). A conserved family of prolyl-4-hydroxylases that modify HIF. *Science (80-.).* **294**, 1337–1340.

Cederblad, G., Carlin, J. I., Constantin-Teodosiu, D., Harper, P. and Hultman, E. (1990). Radioisotopic assays of CoASH and carnitine and their acetylated forms in human skeletal muscle. *Anal. Biochem.* **185**, 274–278.

Cheviron, Z. A., Bachman, G. C., Connaty, A. D., McClelland, G. B. and Storz, J. F. (2012). Regulatory changes contribute to the adaptive enhancement of thermogenic capacity in high-altitude deer mice. *Proc. Natl. Acad. Sci.* **109**, 8635–8640.

Constantin-Teodosiu, D., Cederblad, G. and Hultman, E. (1991). A sensitive radioisotopic assay of pyruvate dehydrogenase complex in human muscle tissue. *Anal.Biochem.* **198**, 347–351.

Cooper, M. B., Forte, C. A. and Jones, D. A. (1986). Citrate interference with the determination of acetylcarnitine: A method for its elimination. *Clin. Chim. Acta* **159**, 291–299.

Cori, G. T. and Green, A. A. (1943). Crystalline muscle phosphorylase: II. Prosthetic group. *J. Biol. Chem.* **151**, 31–38.

Denton, R. M. and Randle, P. J. (1966). Citrate and the regulation of adipose-tissue phosphofructokinase. *Biochem. J.* **100**, 420–423.

Denton, R. M., Randle, P. J. and Martin, B. R. (1972). Stimulation by Calcium Ions of Pyruvate Dehydrogenase Phosphate Phosphatase. *Biochem. J.* **128**, 161–163.

Dubouchaud, H., Butterfield, G. E., Wolfel, E. E., Bergman, B. C. and Brooks, G. a (2000). Endurance training, expression, and physiology of LDH, MCT1, and MCT4 in human skeletal muscle. *Am. J. Physiol. Endocrinol. Metab.* **278**, 571–579.

Dunford, E. C., Herbst, E. a, Jeoung, N. H., Gittings, W., Inglis, J. G., Vandenboom, R., LeBlanc, P. J., Harris, R. a and Peters, S. J. (2011). PDH activation during in vitro muscle contractions in PDH kinase 2 knockout mice: effect of PDH kinase 1 compensation. *Am. J. Physiol. Regul. Integr. Comp. Physiol.* **300**, R1487-93.

Exton, J. H., Friedmann, N., Wong, E. H.-A., Brineaux, J. P., Corbin, J. D. and Park, C. R. (1972). Interaction of glucocorticoids with glucagon and epinephrine in the control of gluconeogenesis and glycogenolysis in liver and of lipolysis in adipose tissue. *J. Biol. Chem.* **247**, 3579–3588.

Fueger, P. T., Hess, H. S., Posey, K. A., Bracy, D. P., Pencek, R. R., Charron, M. J. and Wasserman, D. H. (2004a). Control of exercise-stimulated muscle glucose uptake by GLUT4 is dependent on glucose phosphorylation capacity in the conscious mouse. *J. Biol. Chem.* **279**, 50956–50961.

Fueger, P. T., Hess, H. S., Bracy, D. P., Pencek, R. R., Posey, K. A., Charron, M. J. and Wasserman, D. H. (2004b). Regulation of insulin-stimulated muscle glucose uptake in the conscious mouse: Role of glucose transport is dependent on glucose phosphorylation capacity. *Endocrinology* **145**, 4912–4916.

Fueger, P. T., Bracy, D. P., Malabanan, C. M., Pencek, R. R. and Wasserman, D. H. (2004c). Distributed control of glucose uptake by working muscles of conscious mice: Roles of transport and phosphorylation. *Am. J. Physiol. - Endocrinol. Metab.* **286**, 77–84.

Fueger, P. T., Shearer, J., Krueger, T. M., Posey, K. A., Bracy, D. P., Heikkinen, S., Laakso, M., Rottman, J. N. and Wasserman, D. H. (2005). Hexokinase II protein content is a determinant of exercise endurance capacity in the mouse. *J Physiol* **566**, 533–541.

Ginouvès, A., Ilc, K., Macías, N., Pouysségur, J. and Berra, E. (2008). PHDs overactivation during chronic hypoxia "desensitizes" HIFα and protects cells from necrosis. *Proc. Natl. Acad. Sci. U. S. A.* **105**, 4745–4750.

Goodyear, L. J., King, P. A., Hirshman, M. F., Thompson, C. M., Horton, E. D. and Horton, E. S. (1990). Contractile activity increases plasma membrane glucose transporters in absence of insulin. *Am. J. Physiol. - Endocrinol. Metab.* **258**, E667–E672.

Goodyear, L. J., Hirshman, M. F. and Horton, E. S. (1991). Exercise-induced translocation of skeletal muscle glucose transporters. *Am. J. Physiol. Metab.* **261**, E795–E799.

Guarnera, E. and Berezovsky, I. N. (2016). Allosteric sites: Remote control in regulation of protein activity. *Curr. Opin. Struct. Biol.* **37**, 1–8.

Haman, F. and Blondin, D. P. (2017). Shivering thermogenesis in humans: Origin, contribution and metabolic requirement. *Temperature* **4**, 217–226.

Hardy, K. M., Dillaman, R. M., Locke, B. R. and Kinsey, S. T. (2009). A skeletal muscle model of extreme hypertrophic growth reveals the influence of diffusion on cellular design. *Am. J. Physiol. - Regul. Integr. Comp. Physiol.* **296**, 1855–1867.

Harris, R. A., Bowker-Kinley, M. M., Huang, B. and Wu, P. (2002). Regulation of the activity of the pyruvate dehydrogenase complex. *Adv.Enzyme Regul.* **42**, 249–259.

Hayes, J. P. and O'Connor, C. S. (1999). Natural selection on thermogenic capacity of

high-altitude deer mice. *Evolution (N. Y).* **53**, 1280–1287.

Herbst, E. A. F., Dunford, E. C. E., Harris, R. A., Vandenboom, R., LeBlanc, P. J., Roy, B. D., Jeoung, N. H. and Peters, S. J. (2012). Role of pyruvate dehydrogenase kinase 4 in regulating PDH activation during acute muscle contraction. *Appl. Physiol. Nutr. Metab.* **37**, 48–52.

Herbst, E. A. F., MacPherson, R. E. K., LeBlanc, P. J., Roy, B. D., Jeoung, N. H., Harris, R. A. and Peters, S. J. (2014). Pyruvate dehydrogenase kinase-4 contributes to the recirculation of gluconeogenic precursors during postexercise glycogen recovery. *Am. J. Physiol. Integr. Comp. Physiol.* **306**, R102–R107.

Hochachka, P. W. (1985). Fuels and pathways as designed for support of muscle work. *J. Exp. Biol.* **115**, 149–164.

Hochachka, P. W. (1994). *Muscles as Molecular and Metabolic Machines*. CRC Press.

Hochachka, P. W. and Matheson, G. O. (1992). Regulating ATP turnover rates over broad dynamic work ranges in skeletal muscles. *J. Appl. Physiol.* **73**, 1697–1703.

Hochachka, P. W., Stanley, C., Merkt, J. and Sumar-Kalinowski, J. (1982). Metabolic meaning of elevated levels of oxidative enzymes in high altitude adapted animals: an interpretive hypothesis. *Respir. Physiol.* 303–313.

Hochachka, P. W., Beatty, C. L., Burelle, Y., Trump, M. E., McKenzie, D. C. and Matheson, G. O. (2002). The lactate paradox in human high-altitude physiological performance. *News Physiol. Sci.* **17**, 122–126.

Holden, J. E., Stone, C. K., Clark, C. M., Brown, W. D., Nickles, R. J., Stanley, C. and Hochachka, P. W. (1995). Enhanced cardiac metabolism of plasma glucose in high-altitude natives: Adaptation against chronic hypoxia. *J. Appl. Physiol.* **79**, 222–228.

Howlett, R. a, Parolin, M. L., Dyck, D. J., Hultman, E., Jones, N. L., Heigenhauser, G. J. and Spriet, L. L. (1998). Regulation of skeletal muscle glycogen phosphorylase and PDH at varying exercise power outputs. *Am. J. Physiol.* **275**, R418–R425.

Hultman, E. and Sjöholm, H. (1983). Energy metabolism and contraction force of human skeletal muscle in situ during electrical stimulation. *J. Physiol.* **345**, 525–532.

Ivy, C. M. and Scott, G. R. (2017). Control of breathing and ventilatory acclimatization to hypoxia in deer mice native to high altitudes. *Acta Physiol.* 1–17.

James, D. E., Brown, R., Navarro, J. and Pilch, P. F. (1988). Insulin-regulatable tissues express a unique insulin-sensitive glucose transport protein. *Nature* **333**, 183–185.

Jeoung, N. H. and Harris, R. A. (2008). Pyruvate dehydrogenase kinase-4 deficiency lowers blood glucose and improves glucose tolerance in diet-induced obese mice. *Am J Physiol Endocrinol Metab* **295**, E46–E54.

Juel, C. and Halestrap, A. P. (1999). Lactate transport in skeletal muscle - Role and regulation of the monocarboxylate transporter. *J. Physiol.* **517**, 633–642.

Kacser, H., Burns, J. A. and Fell, D. A. (1995). The control of flux. *Biochem. Soc. Trans.* **23**, 341–366.

Kayser, B. (1996). Lactate during exercise at high altitude. *Eur. J. Appl. Physiol. Occup. Physiol.* **74**, 195–205.

Kim, J. W., Tchernyshyov, I., Semenza, G. L. and Dang, C. V. (2006). HIF-1-mediated expression of pyruvate dehydrogenase kinase: A metabolic switch required for cellular adaptation to hypoxia. *Cell Metab.* **3**, 177–185.

Korotchkina, L. G. and Patel, M. S. (2001). Site specificity of four pyruvate dehydrogenase kinase isoenzymes toward the three phosphorylation sites of human pyruvate dehydrogenase. *J. Biol. Chem.* **276**, 37223–37229.

Kristensen, D. E., Albers, P. H., Prats, C., Baba, O., Birk, J. B. and Wojtaszewski, J. F. P. (2015). Human muscle fibre type-specific regulation of AMPK and downstream targets by exercise. *J. Physiol.* **593**, 2053–2069.

Larsen, S., Nielsen, J., Hansen, C. N., Nielsen, L. B., Wibrand, F., Stride, N., Schroder, H. D., Boushel, R., Helge, J. W., Dela, F., et al. (2012). Biomarkers of mitochondrial content in skeletal muscle of healthy young human subjects. *J. Physiol.* **590**, 3349–3360.

Lau, D. S., Connaty, A. D., Mahalingam, S., Wall, N., Cheviron, Z. A., Storz, J. F., Scott, G. R. and McClelland, G. B. (2017). Acclimation to hypoxia increases carbohydrate use during exercise in high-altitude deer mice. *Am. J. Physiol. - Regul. Integr. Comp. Physiol.* **312**, R400–R411.

Le Moine, C. M. R., Morash, A. J. and McClelland, G. B. (2011). Changes in HIF-1 protein, pyruvate dehydrogenase phosphorylation, and activity with exercise in acute and chronic hypoxia. *AJP Regul. Integr. Comp. Physiol.* **301**, R1098–R1104.

Linn, T. C., Pettit, F. H. and Reed, L. J. (1969). a-Keto acid dehydrogenase complexes, X. Regulation of the activity of the pyruvate dehydrogenase complex from beef kidney mitochondria by phosphorylation and dephosphorylation. *Proc. Natl. Acad. Sci.* **62**, 234–241.

Lui, M. A., Mahalingam, S., Patel, P., Connaty, A. D., Ivy, C. M., Cheviron, Z. A., Storz, J. F., McClelland, G. B. and Scott, G. R. (2015). High-altitude ancestry and hypoxia acclimation have distinct effects on exercise capacity and muscle phenotype

in deer mice. *Am. J. Physiol. Regul. Integr. Comp. Physiol.* **308**, R779–R791.

MacIntosh, B. R., Esau, S. P., Holash, R. J. and Fletcher, J. R. (2011). Procedures for rat in situ skeletal muscle contractile properties. *J. Vis. Exp.* 1–6.

Mahalingam, S., McClelland, G. B. and Scott, G. R. (2017). Evolved changes in the intracellular distribution and physiology of muscle mitochondria in high-altitude native deer mice. *J. Physiol.* **595**, 4785–4801.

McClelland, G. B. and Brooks, G. A. (2002). Changes in MCT 1, MCT 4, and LDH expression are tissue specific in rats after long-term hypobaric hypoxia. *J. Appl. Physiol.* **92**, 1573–1584.

McClelland, G. B. and Scott, G. R. (2019). Evolved mechanisms of aerobic performance and hypoxia resistance in high-altitude natives. *Annu. Rev. Physiol.* **81**, 561–583.

McClelland, G. B., Hochachka, P. W. and Weber, J. M. (1998). Carbohydrate utilization during exercise after high-altitude acclimation: a new perspective. *Proc. Natl. Acad. Sci. U. S. A.* **95**, 10288–10293.

McClelland, G. B., Lyons, S. A. and Robertson, C. E. (2017). Fuel use in mammals: Conserved patterns and evolved strategies for aerobic locomotion and thermogenesis. *Integr. Comp. Biol.* **57**, 231–239.

McDonald, K. S., Delp, M. D. and Fitts, R. H. (1992). Fatigability and blood flow in the rat gastrocnemius-plantaris-soleus after hindlimb suspension. *J. Appl. Physiol.* **73**, 1135–1140.

Meyer, C. W., Willershäuser, M., Jastroch, M., Rourke, B. C., Fromme, T., Oelkrug, R., Heldmaier, G. and Klingenspor, M. (2010). Adaptive thermogenesis and thermal conductance in wild-type and UCP1-KO mice. *Am. J. Physiol. Integr. Comp. Physiol.* **299**, R1396–R1406.

Modak, J., Deckwer, W. D. and Zeng, A. P. (2002). Metabolic control analysis of eucaryotic pyruvate dehydrogenase multienzyme complex. *Biotechnol. Prog.* **18**, 1157–1169.

Natarajan, C., Hoffmann, F. G., Lanier, H. C., Wolf, C. J., Cheviron, Z. A., Spangler, M. L., Weber, R. E., Fago, A. and Storz, J. F. (2015). Intraspecific polymorphism, interspecific divergence, and the origins of function-altering mutations in deer mouse hemoglobin. *Mol. Biol. Evol.* **32**, 978–997.

Nespolo, R. F., Opazo, J. C., Rosenmann, M. and Bozinovic, F. (1999). Thermal acclimation, maximum metabolic rate, and nonshivering thermogenesis of Phyllotis xanthopygus (Rodentia) in the Andes mountains. *J. Mammal.* **80**, 742–748.

Papandreou, I., Cairns, R. A., Fontana, L., Lim, A. L. and Denko, N. C. (2006). HIF-1 mediates adaptation to hypoxia by actively downregulating mitochondrial oxygen consumption. *Cell Metab.* **3**, 187–197.

Pettit, F. H., Pelley, J. W. and Reed, L. J. (1975). Regulation of pyruvate dehydrogenase kinase and phosphatase by acetyl-CoA/CoA and NADH/NAD Ratios. *Biochem. Biophys. Res. Commun.* **65**, 575–582.

Putman, C. T., Spriet, L. L., Hultman, E., Lindinger, M. I., Lands, L. C., McKelvie, R. S., Cederblad, G., Jones, N. L. and Heigenhauser, G. J. (1993). Pyruvate dehydrogenase activity and acetyl group accumulation during exercise after different diets. *Am. J. Physiol.* **265**, E752–E760.

Rahimi, Y., Camporez, J.-P. G., Petersen, M. C., Pesta, D., Perry, R. J., Jurczak, M. J., Cline, G. W. and Shulman, G. I. (2014). Genetic activation of pyruvate dehydrogenase alters oxidative substrate selection to induce skeletal muscle insulin resistance. *Proc. Natl. Acad. Sci.* **111**, 16508–16513.

Rapoport, T. A., Heinrich, R., Jacobasch, G. and Rapoport, S. (1974). A linear steady-state treatment of enzymatic chains: A mathematical model of glycolysis of human erythrocytes. *Eur. J. Biochem.* **42**, 107–120.

Rassier, D. E. and MacIntosh, B. R. (2002). Length-dependent twitch contractile characteristics of skeletal muscle. *Can. J. Physiol. Pharmacol.* **80**, 993–1000.

Rennie, M. J., Edwards, R. H. T., Krywawych, S., Davies, C. T. M., Halliday, D., Waterlow, J. C. and Millward, D. J. (1981). Effect of exercise on protein turnover in man. *Clin. Sci.* **61**, 627–639.

Schippers, M. P., Ramirez, O., Arana, M., Pinedo-Bernal, P. and McClelland, G. B. (2012). Increase in carbohydrate utilization in high-altitude andean mice. *Curr. Biol.* **22**, 2350–2354.

Schippers, M.-P., LeMoine, C. M. R. and McClelland, G. B. (2014). Patterns of fuel use during locomotion in mammals revisited: the importance of aerobic scope. *J. Exp. Biol.* **217**, 3193–3196.

Scott, G. R., Elogio, T. S., Lui, M. A., Storz, J. F. and Cheviron, Z. A. (2015). Adaptive modifications of muscle phenotype in high-altitude deer mice are associated with evolved changes in gene regulation. *Mol. Biol. Evol.* **32**, 1962–1976.

Segal, S. S. and Faulkner, J. A. (1985). Temperature-dependent physiological stability of rat skeletal muscle in vitro. *Am. J. Physiol. - Cell Physiol.* **248**, C265–C270.

Siess, E. A., Brocks, D. G. and Wieland, O. H. (1976). A sensitive and simple method for the study of oxaloacetate compartmentation in isolated hepatocytes. *FEBS Lett.* **70**, 51–55.

Smith, P. K., Krohn, R. I., Hermanson, G. T., Mallia, A. K., Gartner, F. H., Provenzano, M. D., Fujimoto, E. K., Goeke, N. M., Olson, B. J. and Klenk, D. C. (1985). Measurement of Protein Using Bicinchoninic Acid. *Anal. Biochem.* **150**, 76–85.

Spriet, L. L. and Heigenhauser, G. J. F. (2002). Regulation of Pyruvate Dehydrogenase (PDH) Activity in Human Skeletal Muscle During Exercise. *Exerc. Sport Sci. Rev.* **30**, 91–95.

Suarez, R. K. and Moyes, C. D. (2012). Metabolism in the age of "omes." *J. Exp. Biol.* **215**, 2351–2357.

Suarez, R. K., Darveau, C. A. and Hochachka, P. W. (2005). Roles of hierarchical and metabolic regulation in the allometric scaling of metabolism in Panamanian orchid bees. *J. Exp. Biol.* **208**, 3603–3607.

Sugden, M. C. and Holness, M. J. (2006). Mechanisms underlying regulation of the expression and activities of the mammalian pyruvate dehydrogenase kinases. *Arch. Physiol. Biochem.* **112**, 139–149.

Sugden, M. C., Bulmer, K. and Holness, M. J. (2001). Fuel-sensing mechanisms integrating lipid and carbohydrate utilization. *Biochem. Soc. Trans.* **29**, 272–278.

Sylow, L., Kleinert, M., Richter, E. A. and Jensen, T. E. (2017). Exercise-stimulated glucose uptake-regulation and implications for glycaemic control. *Nat. Rev. Endocrinol.* **13**, 133–148.

Tate, K. B., Ivy, C. M., Velotta, J. P., Storz, J. F., McClelland, G. B., Cheviron, Z. A. and Scott, G. R. (2017). Circulatory mechanisms underlying adaptive increases in thermogenic capacity in high-altitude deer mice. *J. Exp. Biol.* **220**, 3616–3620.

Taylor, R. C., Weibel, E. R., Weber, J.-M., Vock, R., Hoppeler, H., Roberts, T. J. and Brichon, G. (1996). Design of the oxygen and substrate pathways. I. Model and Strategy to Test Symmorphosis in a Network Structure. *J. Exp. Biol.* **199**, 1643–1649.

Templeman, N. M., Schutz, H., Garland, T. and McClelland, G. B. (2012). Do mice bred selectively for high locomotor activity have a greater reliance on lipids to power submaximal aerobic exercise? *Am. J. Physiol. - Regul. Integr. Comp. Physiol.* **303**, 101–111.

Towbin, H., Staehelin, T. and Gordon, J. (1979). Electrophoretic transfer of proteins from polyacrylamide gels to nitrocellulose sheets: Procedure and some applications. *Proc. Natl. Acad. Sci. U. S. A.* **76**, 4350–4354.

Trump, M. E., Heigenhauser, G. J. F., Putman, C. T. and Spriet, L. L. (1996). Importance of muscle phosphocreatine during intermittent maximal cycling. *J. Appl.*

Physiol. **80**, 1574–1580.

Vacanti, N. M., Divakaruni, A. S., Green, C. R., Parker, S. J., Henry, R. R., Ciaraldi, T. P., Murphy, A. N. and Metallo, C. M. (2014). Regulation of substrate utilization by the mitochondrial pyruvate carrier. *Mol. Cell* **56**, 425–435.

Wasserman, D. H. (2008). Four grams of glucose. *Am. J. Physiol. Metab.* **296**, E11–E21.

Wasserman, D. H., Kang, L., Ayala, J. E., Fueger, P. T. and Lee-Young, R. S. (2011). The physiological regulation of glucose flux into muscle in vivo. *J. Exp. Biol.* **214**, 254–262.

Weber, J.-M. (2011). Metabolic fuels: regulating fluxes to select mix. *J. Exp. Biol.* **214**, 286–294.

Weber, J.-M. and Haman, F. (2004). Oxidative fuel selection : adjusting mix and flux to stay alive. *Int. Congr. Ser.* **1275**, 22–31.

Weber, J. M., Roberts, T. J., Vock, R., Weibel, E. R. and Taylor, C. R. (1996). Design of the oxygen and substrate pathways. III. Partitioning energy provision from carbohydrates. *J. Exp. Biol.* **199**, 1659–66.

Weibel, E. R. and Hoppeler, H. H. (2005). Exercise-induced maximal metabolic rate scales with muscle aerobic capacity. *J. Exp. Biol.* **208**, 1635–1644.

Weibel, E. R., Taylor, C. R. and Hoppeler, H. (1991). The concept of symmorphosis: A testable hypothesis of structure-function relationship. *Proc. Natl. Acad. Sci. U. S. A.* **88**, 10357–10361.

Welch, K. C., Altshuler, D. L. and Suarez, R. K. (2007). Oxygen consumption rates in hovering hummingbirds reflect substrate-dependent differences in P/O ratios: carbohydrate as a "premium fuel." *J. Exp. Biol.* **210**, 2146–2153.

Wilson, J. E., Sacktor, B. and Tiekert, C. G. (1967). In situ regulation of glycolysis in tetanized cat skeletal muscle. *Arch. Biochem. Biophys.* **120**, 542–546.

Wu, J. L., Wu, Q. P., Huang, J. M., Chen, R., Cai, M. and Tan, J. B. (2007). Effects of L-malate on physical stamina and activities of enzymes related to the malate-aspartate shuttle in liver of mice. *Physiol. Res.* **56**, 213–220.

Yeaman, S. J., Hutcheson, E. T., Roche, T. E., Pettit, F. H., Brown, J. R., Reed, L. J., Watson, D. C. and Dixon, G. H. (1978). Sites of phosphorylation on pyruvate dehydrogenase from bovine kidney and heart . *Biochemistry* **17**, 2364–2370.

Appendix

Table A.1. Contractile characteristics of gastrocnemius stimulated *in situ*. Max force production (F_{max}), average force production during a submaximal workload (F_{work}) reported as absolute force (in mN). Relative work force production standardized to F_{max}. Optimal length (L_o) reported as absolute length. Fatigue reported as average force of final three contractions standardized to average force of initial three contractions (F_{in}). Data presented as mean ± SEM. N = 5-8.

	Normoxia		Hypoxia	
	Light	Heavy	Light	Heavy
F_{max} (mN)	474.4 ± 59.7	408.1 ± 45.1	427.9 ± 36.3	371.4 ± 20.5
F_{work} (mN)	106.4 ± 18.1	198.6 ± 20.5	96.1 ± 9.3	176.1 ± 10.0
Rel. F_{work} (%F_{max})	22.3 ± 2.4	49.2 ± 1.4	22.4 ± 0.8	47.6 ± 1.4
L_o (mm)	10.1 ± 0.2	11 ± 0.6	11.1 ± 0.5	10.7 ± 0.5
Fatigue (%F_{in})	96.6 ± 4.9	92.1± 5.4	94.9 ± 3.0	92.8 ± 1.9

Fig. A.1. Sample force frequency curve of a gastrocnemius stimulated *in situ*.

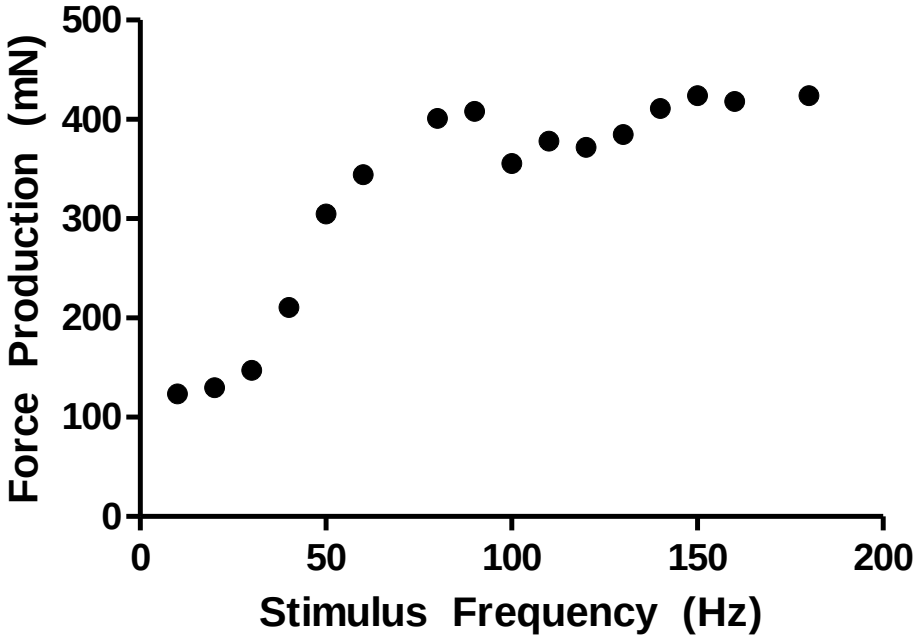
Force Production (mN)
500
400
300
200
100
0
0
50
100
150
200
Stimulus Frequency (Hz)

Fig. A.2. Sample standard curve for PDH assay. Counts per minute (CPM) of ^{14}C-citrate produced from known concentrations of acetyl-CoA assayed in duplicate using a radiolabelled assay.

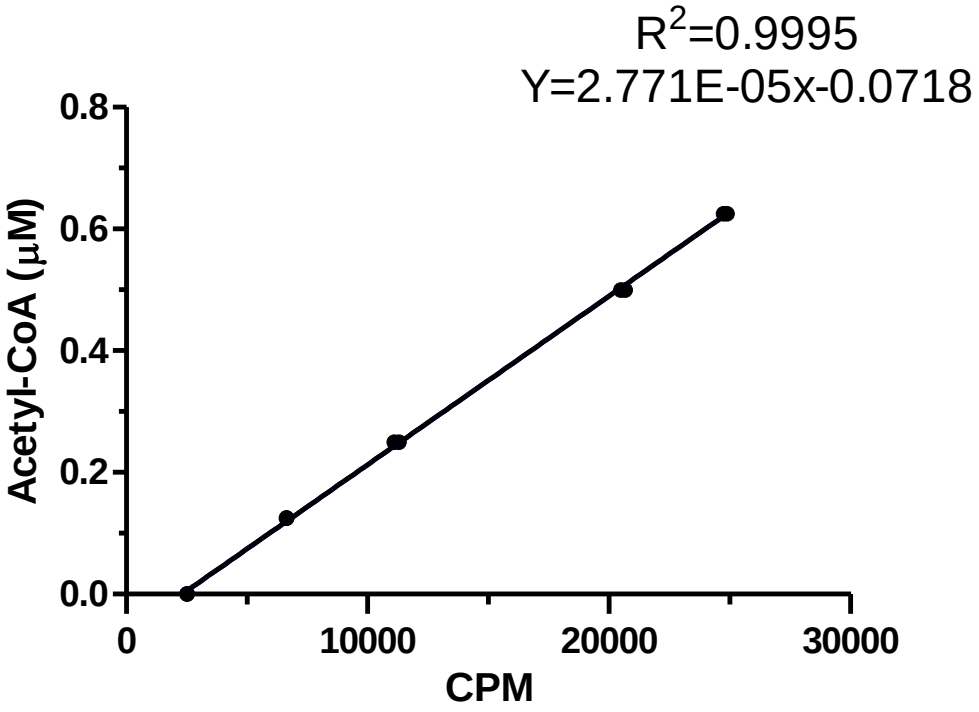
R2=0.9995
Y=2.771E-05x-0.0718
Acetyl-CoA (µM)
0.0
0.2
0.4
0.6
0.8
0
10000
20000
30000
CPM

Table A.2. Dilution factors used for calculation of PDH activity. A) dilution factors for the homogenization and PDH reaction steps. B) dilution factors for acetyl-CoA extracts prior to acetyl-CoA assay. *represents values that are variable: K_2CO_3 volume ranges from 12 to 14 µL; corresponding dilution factor ranges from 1.26 to 1.27.

A

	Dilution	Dilution Factor
Homogenization	(30µL + 1mg) / 1mg	31
PDH Reaction	(30µL + 720µL) / 30 µL	26
Acetyl-CoA Extract	(200µL + 40µL + 13*µL) / 200µL	1.265*
Acetyl-CoA Dilution	(10µL + 190µL) / 10µL **	20**

B

	Rest		Exercise	
	PDHa	PDHt	PDHa	PDHt
Normoxic G_1	10	40	40	40
Hypoxic G_1	10	40	40	40
Wild	20	40	40	40